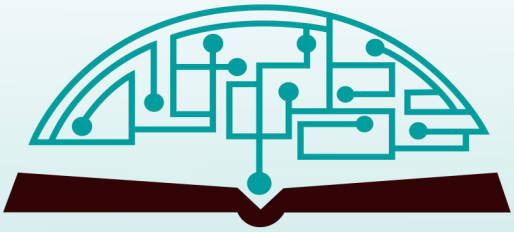

IJHSR International Journal of High School Research

September 2019 | Volume 1 | Issue 2
ijhighschoolresearch.org

ACASU

American Commission for Accreditation of Schools and Universities

ACASU promotes school environments that enable students to develop **Lifetime Qualities** that assist graduates in making the world a better place.

STANDARDS

* Governance
* Education
* Culture
* Operations
* Quality

ACASU BENEFITS

Enhances your institution's reputation and garners the esteem of Americans.

Assures students and their families that your institution meets American standards for high quality education.

Shows students and parents your institution's commitment to success and your ability to perform at high quality educational standards.

Shows your colleagues and the general public that your institution has a genuine interest in institutional improvement.

Sets your institution apart as a leader among others.

Provides you with a network of skilled professionals and resources to assist meeting your accreditation, enrollment, and college attainment goals.

Ensures that your standard operating procedures are compliant with U.S. international student regulations.

Provides you a network of high quality schools, universities, and administrators from around the world to learn from and to partner with in global activities.

OUR MISSION

Endorse the highest quality education for students for lifetime achievement and service to others in a connected world.

Accreditation is a recognized status and a process used to promote high quality education and continuous improvement. It is a level of prestige earned by a school or university that has met or exceeded set criteria of educational quality.

For more information, visit acasu.org

GENIUS OLYMPIAD

www.geniusolympiad.org

International Environmental Project Fair for Grades 9-12

Project Categories Include:

Science
Business
Visual and Performing Arts
Writing
Robotics

June 2020

Oswego, New York, USA

geniusolympiad.org

Apply: December 15 to March 11

Table of Contents

September 2019 | Volume 1 | Issue 2

Editorial Board

International Journal of High School Research

IJHSR

ijhighschoolresearch.org

Implication of the inflammasome protein complex in the autoimmune lymphoproliferative syndrome (ALPS)

Tali Finger
1. Scheck Hillel Community School, 19000 NE 25th Avenue, North Miami Beach, Florida, 33180, United States
2. Alef Peretz, Rua Angelina Vita 450, São Paulo, SP, 01455-070, Brazil

tafinger2021@ehillel.org

ABSTRACT: Autoimmune diseases are chronic diseases that affect 5% to 8% of the world's population. Exploring, in-depth, a specific autoimmune disease such as the autoimmune lymphoproliferative syndrome (ALPS) may help broaden our knowledge of all forms of autoimmune diseases. Our research project consisted of two parts. We first reported a case of a patient with a possible autoimmune disorder in the spectrum of ALPS-like disorders. We then suggested the implication of a protein complex called the Inflammasome in ALPS and investigated the yet unclear interaction between innate immunity and cellular apoptosis. We used systems biology tools, such as Ingenuity® and Cytoscape®. These analyses showed that: 1) the studied patient report fits the ALPS spectrum, which is, therefore, significantly broader than that described in the literature; 2) the Inflammasome is indeed implicated in the reported case; and 3) ALPS is not only involved in the organism's adaptive immunity as it was believed but is also in the organism's innate immunity; 4) the relationship between innate immunity and cellular apoptosis is broader than previously thought. The study's findings provide new insights on these disorders and may help elucidate mechanisms implicated in autoimmune diseases, and thus contribute to the development of more effective treatments.

KEYWORDS: Immunology; Innate; Immunity; Apoptosis; ALPS; Inflammasome

Introduction. Innate immunity is the invader's first contact with the organism, and is formed by i) physical barriers such as the skin; ii) cellular factors including phagocytes (macrophages, neutrophils, and mast cells), dendritic cells, and NK (Natural Killer) cells; iii) molecular factors such as cytokines (molecules that emit signals between cells during the immune response), chemokines (molecules that recruit lymphocytes to lymphoid tissues and inflammation sites), complement proteins (molecules responsible for amplifying phagocytosis and inflammation, in addition to killing some types of pathogens), and acute phase proteins (molecules that help phagocytosis and complement system activation).

The innate immune response in an organism begins when one of its cells recognizes a pathogen-associated molecular pattern (PAMP). PAMPs are structures that are essential for microorganism survival and are absent in healthy, malignant and microorganism-free humans. Some examples include flagellin, the main component of the bacterial flagellum, and double-stranded RNA, found in some viruses. The first reaction of the IS to PAMPs is phagocytosis, a process by which the cell engulfs a microorganism in order to destroy it. The second reaction is the production of pro-inflammatory cytokines, which stimulates the cells that line the interior surface of blood vessels to express selectins (adhesion molecules). These molecules promote a weak adhesion between circulating lymphocytes and the interior surface of blood vessels that, with the force exerted by the blood, carry lymphocytes to the inflammation site. [1] In addition to cytokine production, chemokines are produced in the inflammation site to attract more lymphocytes to help fight pathogens. Besides cellular recruitment, resident cells of the inflammation site produce mediators that promote vasodilatation and increase the permeability of the walls of blood vessels causing blood to accumulate at the infection site, which facilitates microorganism elimination. [2]

ALPS is a very rare and severe condition caused by a deficiency in lymphocyte apoptosis (programmed cellular death) that is usually caused by a mutation in the FAS gene (FAS cell surface death receptor) responsible for apoptosis-inducing molecules, which play a central role in the physiological regulation of cellular apoptosis.

The patient studied in this case did not present any of the genomic mutations described as associated with the risk of developing ALPS. We used the patient's exome sequencing data to compare the symptoms' molecular cause to the pathways known to be involved with ALPS. However, in our study, we could identify new candidate genes for the disease. We also observed new mechanisms implicated in ALPS, which support our hypothesis of the possible implication of the Inflammasome protein complex in ALPS.

Our study is based on concepts that explore aspects of the immune system (IS), which consists of the coordinated response of cells and molecules against agents which are foreign to the body. The IS can be divided into two categories: innate (or natural) immunity and adaptive (or acquired) immunity.

One of the protein complexes activated during inflammation is the Inflammasome. [3] The Inflammasome is implicated in the regulation of innate immunity and intracellular pathways of programmed cell death. It activates caspases, or proteins that

DOI: here
Reference here

are responsible for deactivating other proteins by breaking down their peptide bonds. Caspases are essential for programmed cell death and cytokine production. [4]

While innate immunity recognizes pathogen-associated patterns, adaptive immunity recognizes specific pathogens. Lymphocytes develop individual receivers that can identify specific epitopes (groups each formed by 5 to 17 amino acids). Each receiver is randomly generated, formed by a random combination of 5 genes with immunologic functions and with unpredictable specificity.

Adaptive immunity responses can be divided into humoral immunity and cellular immunity. The humoral immunity consists of an immune response mediated by molecules through the blood and antibodies found in mucous secretions. Antibodies are produced by B-lymphocytes and are the organism's main defense against pathogens. They recognize and eliminate antigens (foreign particles to the body) and neutralize infectious agents. Cellular immunity, on the other hand, involves an immune response mediated by T-lymphocytes. When microorganisms are able to survive and invade intracellular space, they become unreachable to circulating antibodies. T-lymphocytes promote the destruction of these microorganisms and, if necessary, the infected cell's death.

When a similar pathogen enters the body, there are already many lymphocytes ready to fight it, and it no longer represents a risk to the organism. This feature is called immune memory and is key to the adaptive immunity. [5]

The immune system elicits a destructive response regardless of its target. Such destructiveness explains the severity of immune responses against the body itself, which characterize the so-called autoimmune diseases.

Autoimmune diseases are among the main causes of death by diseases worldwide. However, the underlying mechanisms of these diseases are not fully understood, which represents an obstacle in the development of effective drug treatments for autoimmune diseases. [6]

Our study is based on a case report of a patient whose symptoms were not clearly understood, hampering the establishment of a drug treatment that could effectively improve his/her quality of life.

To our knowledge, this is a unique case in the literature. This is an original study that investigated the implication of the Inflammasome in ALPS through a systems biology approach. The study of the interaction between candidate genes for a specific disease and their biological pathways can help us better understand the underlying mechanisms and interactions of many other similar diseases. It shows autoimmune diseases are closely related and the importance of fully investigating specific cases of these diseases.

The research question that gave rise to this research project was the relationship between a case of a patient with an unidentified autoimmune disease, and ALPS. This relationship was hypothesized based on a case of a 28-year-old male patient who, from a young age, presented with recurrent inflammatory responses due to reasons such age-related acne and tooth loss. At the time, doctors were not able to reach a diagnosis or establish an effective treatment for his condition. Since these inflammatory conditions were not severe, they were not carefully investigated. In February 2006, the patient was treated with nonsteroidal anti-inflammatory drugs (NSAIDs) and had to be immediately hospitalized due to severe diarrhea and epididymitis (inflammation of the epididymis, an organ whose function is to collect and store the sperm produced in the testicles). His condition progressed to ecchymosis (blood infiltration into the tissue mesh) and severe gingival hemorrhage. The initial investigation showed thrombocytopenia (low platelet count in the blood), lymphopenia (decreased quantity of lymphocytes in the blood), and hepatosplenomegaly (enlargement of the liver and the spleen, generally caused by a large immune defense activity of the organism), and test results were negative for infectious, autoimmune, hematological, and neoplastic disorders.

The patient's lack of response to antibiotics suggested a more complex diagnosis. The attending physician cleared the patient and suggested he saw an infectologist for further investigation. In 2008, when the patient was 19, his health remained impaired. Frustrated by the lack of progress in the investigations, he discontinued all medications and clinical follow-ups. He then developed a series of inflammatory conditions in many organs that led to severe systemic inflammation requiring hospitalization in February 2009. Despite vigorous antibiotic therapy, he progressed to severe pneumonitis (inflammation in the lungs) and polyserositis (chronic inflammation of the serous membranes, which cover the body's cavities). Because symptoms worsened rapidly, the patient was transferred to the intensive care unit (ICU). Again, all test results for potential infectious, autoimmune, hematological, and neoplastic disorders using morphological, immunological, molecular, serological, and microbiological investigation techniques failed to identify the source of systemic inflammation.

A month later, while still in the hospital, the patient showed improvement in the pneumonitis. However, in April 2009, he had a series of seizures that required coma induction, mechanical ventilation, and brain monitoring by continuous electroencephalogram (EEG). A week later, the patient was diagnosed with an inflammatory condition in the nervous system, although no pathogens were found. At that time, one of the diagnostic possibilities raised was ALPS.

The first part of this research study aimed to ascertain whether the case studied belonged to the ALPS spectrum using systems biology tools. The second part of the study aimed to assess the relationship between ALPS and the Inflammasome, which may entail new treatment possibilities for both ALPS and the reported case, and to examine whether the link between the body's innate immunity and cellular apoptosis is indeed broader than described in the literature. We based our study on the main notions that: i) genes interact with each other in cellular functions; ii) these interactions can be protein-protein interactions; and iii) genes that interact with each other or have the same function form a system. [7]

This research highlights the importance of studying the relationship between innate immunity and cellular apoptosis

that, we hypothesize, occurs through the Inflammasome. This project sought to achieve three goals using systems biology as the main research tool to investigate a case of a patient with a possible autoimmune disorder: [1] to ascertain whether this case is part of the autoimmune lymphoproliferative syndrome (ALPS) spectrum, a very rare and severe syndrome caused by a deficiency in lymphocyte apoptosis; [2] to understand the relationship between the Inflammasome protein complex and ALPS in the above mentioned case; [3] understand, through the Inflammasome, the relationship between innate immunity and cellular apoptosis.

Results and Discussion. Our results are divided in two parts corresponding to the two phases of the investigation.

4-1 Phase 1 - preliminary gene candidates. This analysis was based on a list of 10 genes. Seven of them have been implicated in ALPS (*FAS, FASLG, CASP8, CASP10, KRAS, NRAS,* and *PRKCD*) (Appendix A), and three were implicated in the reported case (*MEFV, NOD2* and *CASP8AP2)* (Appendix B).

We used the following definitions in our study: i) **seed genes** – genes that are part of the analyzed list (listed above); and ii) **candidate genes** – genes intro-

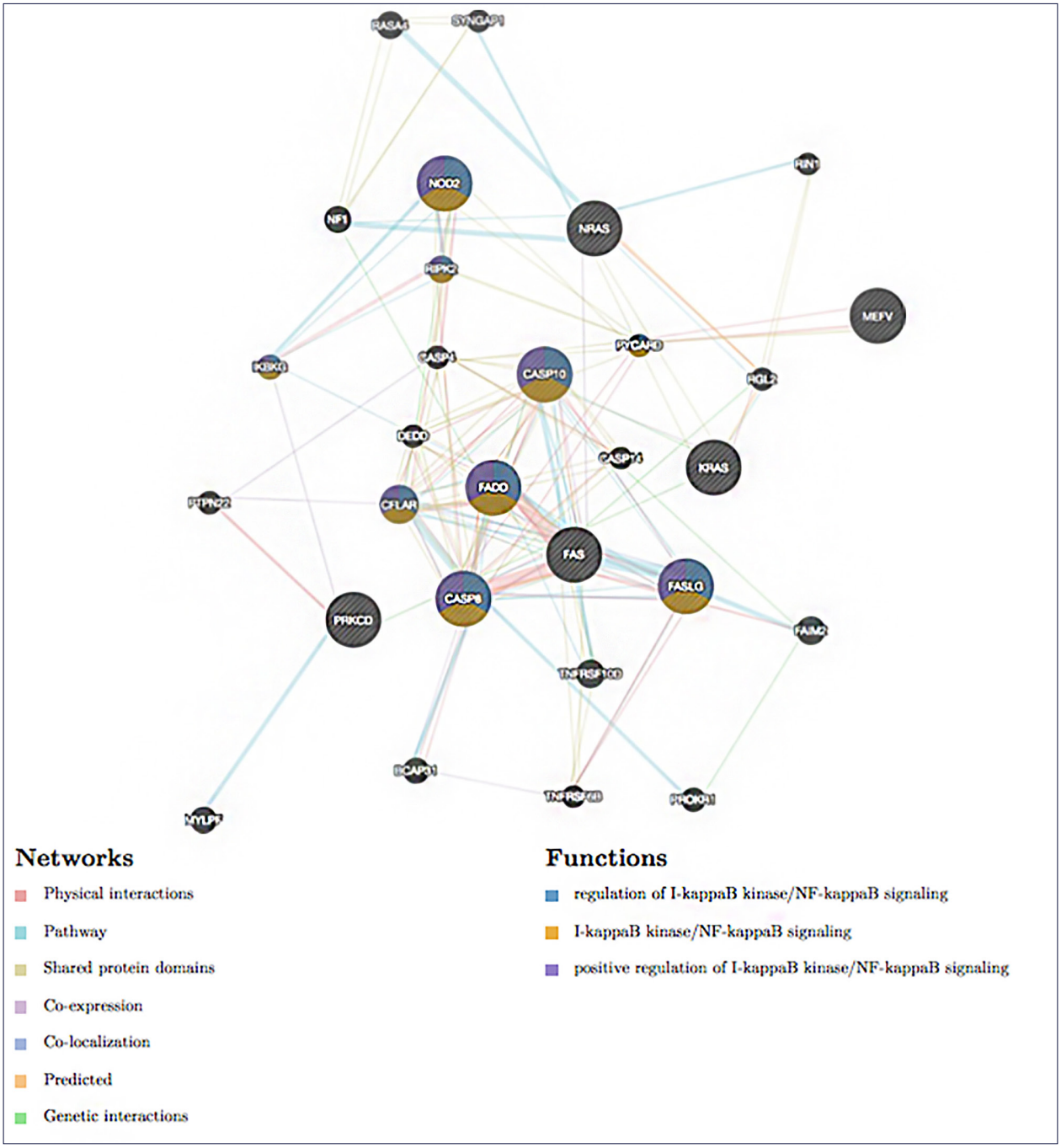

Figure 1. Network 1 generated by GeneMANIA®. The striped nodes are seed genes and the solid ones are candidate genes.

DOI: here
Reference here

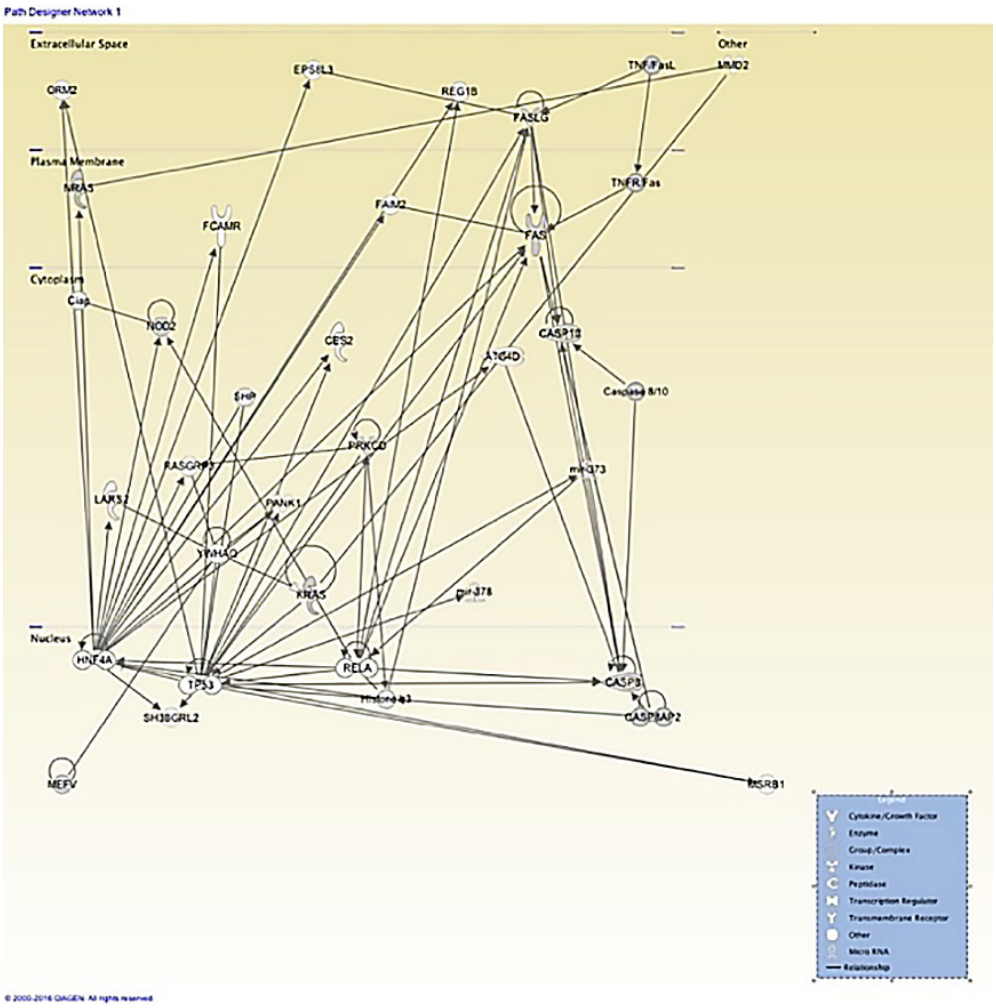

Figure 2. Network 3 generated by Ingenuity®. This picture represents the organization of a cell: the extracellular space, cell membrane, cytoplasm and nucleus. Each symbol represents one protein, and the direction of the arrow indicates the direction of the interaction.

duced to the network because their functions were similar to those of genes implicated in the analyzed list.

Human organisms contain millions of biological pathways that function uninterruptedly. These pathways are results of interactions between proteins. Thus, we primarily studied the interaction between proteins, and then the biological pathways resulting from these interactions.

4-1-1 Interaction Between Proteins. The network of interactions between genes generated using the GeneMANIA® database identified a total of 29 genes, of which 20 were network candidate genes.

Then considering only the physical interactions, the genes were divided into two groups, and 6 candidate genes were found not to be part of network 1 (Figure 1). The first group included the *KRAS, NRAS* and *RGL2* genes, and the second group included the other 5 genes implicated in ALPS, the 2 genes implicated in the reported case identified by GeneMANIA®, and the other 13 network candidate genes. The second group was formed by a total of 32 physical and direct interactions between first neighbors. The genes with the highest amount of physical interactions were *FADD, CASP8* and *CASP10*. When only physical interactions were considered, only the seed genes *PRKCD, KRAS* and *NRAS* did not interact directly with the other ALPS proteins (Figure 1).

When all kinds of interactions were considered, we found that the proteins coded by the genes from the reported case, interacted in the same network with ALPS proteins.

Besides using GeneMANIA® to identify the interaction between genes, we also used Ingenuity® (Figure 2). The criteria used for this network was also the direct interaction between first neighbors. The network generated by Ingenuity® showed 18 candidate genes, in addition to the 10 analyzed genes. The *CASP8AP2* gene, which had not been recognized by GeneMANIA®, was recognized by Ingenuity® and was shown to be directly interacting with *CASP8* from ALPS in the nucleus. Moreover, we could observe where the proteins interact within a cell. *FASLG* is found in the extracellular space, *NRAS* and *FAS* are found in the cell membrane, *NOD2, PRKCD* and *CASP10* are in the cytoplasm and *MEFV, CASP8* and *CASP8AP2* are inside the nucleus. Mutations in genes with nuclear functions can be associated with gene transcription and DNA repair, both important processes in cellular function. All the genes from the reported case were part of the network of ALPS genes.

The protein with the largest amount of interactions was *HNF4A*, a candidate gene found in the nucleus, which regulates the expression of many hepatic genes.[8] This gene is important for the development of the liver, kidneys, and intestines. Some symptoms involving these organs were observed in the reported case and ALPS.

The protein coded by the gene *CASP8* also had many interactions (Figure 1).

4-1-2 Biological Pathways. GeneMANIA® showed that the three main biological pathways involving seed genes were the pathways involving I-kappa B kinase regulation and NF-kappaB signaling. The latter is critical for the immune response to infections, and its faulty regulation can cause many autoimmune diseases. [9] Eight nodes in the network are impli-

cated in these pathways: *NOD2, CASP8, CASP10, PYCARD, FADD, FASLG, RIPK2*, and *CFLAR*. Four of them are seed genes, three of them are implicated in ALPS, and one was found in the reported case (Figure 1).

According to Ingenuity®, the main biological pathway involved with seed genes is the apoptosis signaling pathway. The protein *FASLG* receives a stimulus and activates the *FAS* receiver that in turn recruits the *FADD* adaptor. This adaptor, through *DED* (death effector domain), activates procaspase 8. The *DISC* complex (death signaling inducing complex) is made up of the proteins *FAS, FASLG, FADD* and *DED*. *FADD* activates procaspase[8], which activates CASP8, which is responsible for the cleavage of *CASP3* (Appendix C). *CASP8* is part of a group of caspases called initiator caspases, which are responsible for initiating the apoptosis pathway. *CASP3* is part of another group called executioner caspases, which are responsible for actualizing apoptosis. *CASP8* interacts with *CASP8AP2* in the nucleus, which points to a relationship between the reported case and ALPS.

We also used LEGO®, which prioritizes genes considering their proteins' physical interactions and their role in the over-represented biological pathway. In this analysis, over-represented pathways included apoptosis and *FAS* signaling pathways. The most important genes in these pathways were *CASP8, CASP10* and *FASLG*. These findings confirm the results obtained through GeneMANIA®, where *CASP8* and *CASP10* had the greatest amount of connections, and through Ingenuity®, which also found these three nodes in every over-represented biological pathway.

4-2 Phase 2 - novel gene candidates. As described in Methods, genes with mutations in the reported case were selected in different ways in the first and second phases of the investigation. At the end of the first investigation, after presenting our results to the attending physicians, we had access to the original exome sequencing data and could make a more exact selection of the genes with mutations involved in this case, which included the following genes: *NOD2, MEFV, LIG1, AK2, IFNGR2, CFHR5, UNC13D, CD19, CASP10, DNASE1L3, C8A, MEFV, DCLRE1C, DDX58, TTC37, CFH, MSH6, CD3G, NLRP12, VPREB1, TLR3, IL17RA, SLC29A3, DOCK8, APOL1, FPR1* and *ITGB2* (Appendix C). Thus, in the second investigation, based on the additional information obtained in the first investigation, we could use Cytoscape®, a more complex platform than the previously used ones. This platform generated three different networks. The first one had genes implicated in the reported case; the second one only had genes implicated in ALPS; and the third had genes from both conditions.

This analysis aimed to observe the mechanisms of both conditions in different systems to further support the hypothesis of a connection between the genes and the Inflammasome complex.

Below are the results of the described networks:

4-2-1 Network 1 = genes only implicated in the reported case.

i. GeneMANIA®: The network showed a total of 46 genes, of which 26 were seed genes and 20 candidate genes. The three candidate genes with the greatest score of similarity with the network were *APOL2, DCLRE1B,* and *DCLRE1A*, respectively (Figure 3).

ii. CentiScaPe®: Based on the parameters described in Methods, the main nodes in the network were *LIG1* (highest *bridging*), *AK2* (second highest *bridging*), *SELL* (highest *betweenness* and highest *degree*), *MNDA* (second highest *degree*), and *C1R* (second highest *betweenness*).

iii. MCode®: The network was divided into three different clusters. The first cluster, with 12 nodes and 88 interactions, presented a score of 10,364, and its main biological pathway was inflammatory response; the second cluster, with 11 nodes and 31 interactions, presented a score of 3.6, and its main biological pathway was complement activation; and the third pathway, with 3 nodes and 4 interactions, presented a score of 3, and its main biological pathway was positive regulation of cytokine production. A high score means the cluster is highly interconnected.

4-2-2 Network 2 = genes implicated in ALPS.

i. GeneMANIA®: The network showed 27 genes, of which 7 were seed genes and 20 candidate genes. Among the candidate genes, the ones with the highest scores were *FADD, CFLAR* and *FAIM2*.

ii. CentiScaPe®: The main genes in the network were *FAS* (highest *betweenness* and highest *degree*), *KRAS* (second highest *betweenness*), *CASP8* (second highest *degree*), *PTPN22* (highest *bridging*), and *PRKCD* (second highest *bridging*).

iii. MCode®: The network was divided into 2 clusters. The first cluster showed 9 nodes and 61 interactions, a score of 7 and its main biological pathway was extrinsic apoptosis signaling; the second cluster showed 7 nodes and 10 interactions, a score of 2,667 and its main biological pathway was humoral immune response.

The following discussion is based on a comparison of the protein-protein interaction network analysis with the current literature.

Based on our findings from the first investigation we suggested the hypothesis that the studied case was part of the ALPS spectrum. Our second investigation, which utilized different databases, confirmed the initial hypothesis and suggested new hypotheses to be examined.

In *network 1*, which included genes from the reported case, the main function within the network of the genes with highest *bridging* (*LIG1* and *AK2*) is to connect *MSH6* to the rest of the network. *MSH6* is responsible for DNA repair and has been implicated in some autoimmune diseases such as autoimmune inflammatory myopathy .[10] *LIG1* has been associated with DNA replication and recombination, and *AK2* is responsible for a type of adenylyl cyclase (an enzyme responsible for transforming *ATP* into *AMP*) implicated in cellular apoptosis. As *bridging* measures the degree of a gene's first neighbors, *MSH6* gene possibly has a central role in the network.

In *network 2*, which only included genes implicated in ALPS, *FADD* was shown to be a candidate gene for the net-

DOI: here
Reference here

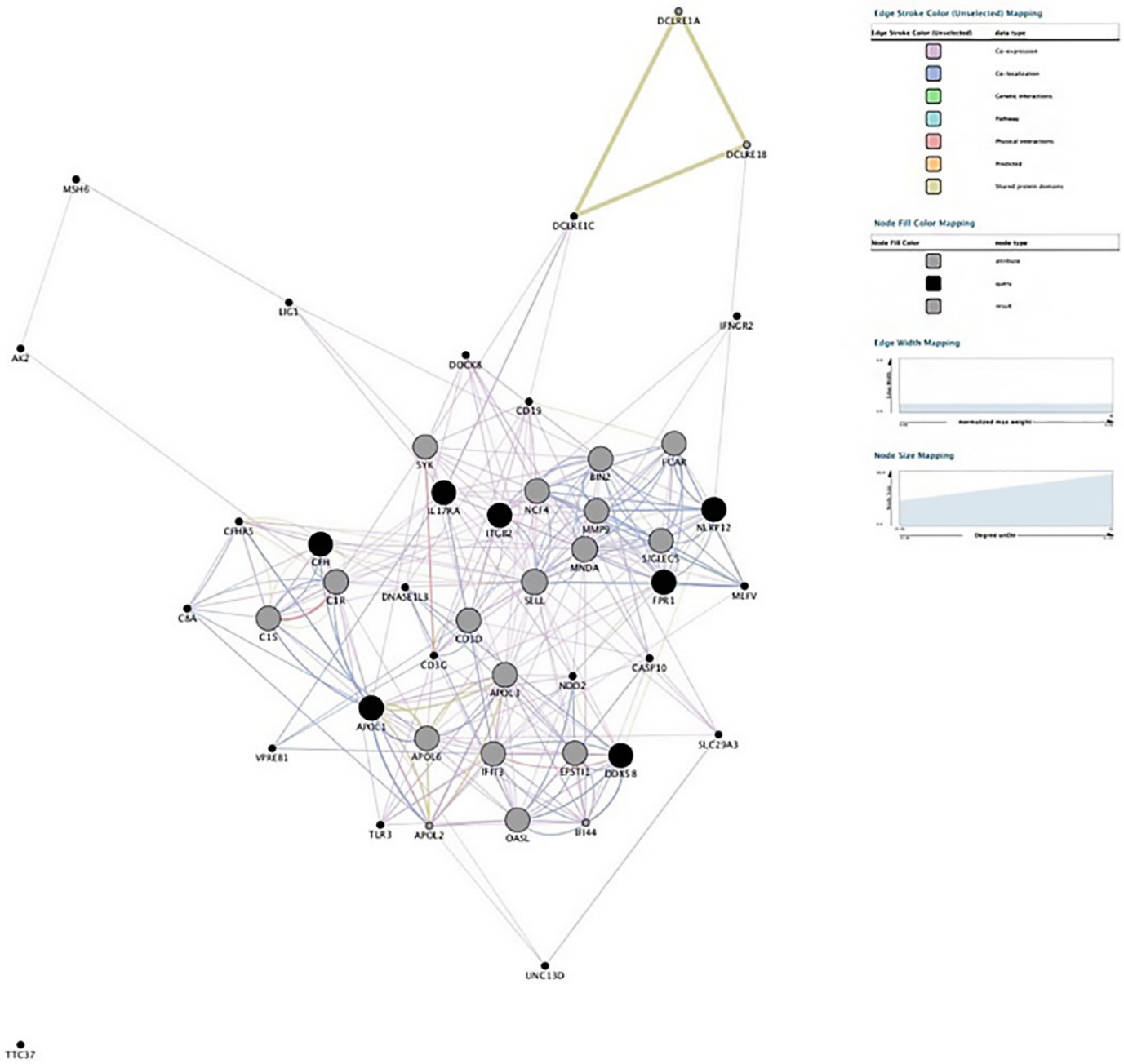

Figure 3. Network 1 generated by GeneMANIA® with information from CentiScaPe® through the Cytoscape® platform.

work with a score of 13.01. This high value shows the node is very important for the network, even though it is not a seed gene. *FADD* has been implicated in some ALPS mechanisms, but so far it has not been considered a possible candidate gene for the syndrome. This finding suggests *FADD* is a candidate gene for ALPS. However, additional studies are needed to confirm this hypothesis.

ASC adaptor, which is essential for the activation of the Inflammasome and tissue homeostasis, has proved to be relevant to the development of autoimmune diseases. In some cells where the Inflammasome has been activated, ASC accumulates in the extracellular space maintaining its ability to control pro-IL-1ß production and prolonging inflammation. There are records in the literature implicating extracellular ASC in different chronic auto-inflammatory diseases. Although it is still being developed, an anti-ASC treatment has successfully reduced the activation of caspase-1 and IL-1ß in a significant number of cases. [11]

In *network 3*, we observed that *CASP8* and *CASP10*, whose roles are clearly related to cellular apoptosis, interacted in the same network as *NOD2, MEFV*, and *NLRP12*, whose functions are essential to innate immunity. *CFLAR* was among the main genes of *network 2*. *CFLAR* has a major role in cellular apoptosis and was shown to be co-expressed with *NOD2*,

one of the main receptors of the Inflammasome and innate immunity. *PROKR1* is implicated in inflammation; however, it showed the second highest bridging of *network 3*, where it connected *CASP8* and *MEFV*. The *DDX58* gene was observed to be in the same protein domain as *MEFV, NOD2,* and *NLRP12*, and interacted physically and directly with the *CASP8* gene.

Conclusion. Our investigation showed that the studied case is part of the ALPS spectrum. This finding gives new insight into the set of available information about this poorly understood disease and about autoimmune diseases in general. Furthermore, we observed that *FADD* is part of the ALPS spectrum, being a candidate gene for the disease.

Before our investigation, the reported case had been associated with adaptive immunity only. However, we found that, besides adaptive immunity, it is also involved in innate immunity mechanisms. Since the case is part of the ALPS spectrum, the syndrome is very likely associated with innate immunity mechanisms, which has never been suggested in the literature.

The hypothesis of the involvement of innate immunity in ALPS was set forward in the main proposal of the project: Implication of the Inflammasome Protein Complex in the Autoimmune Lymphoproliferative Syndrome since the Inflammasome is part of the innate immunity. Our findings support this hypothesis and provide additional information on the subject such as the inclusion of *NLRP12* Inflammasome in the known spectrum, previously limited only to *NLRP3*.

Regarding treatment approaches for the reported case and ALPS, two new fronts have emerged:

i. Given the involvement of the ASC adaptor in the Inflammasome, extracellular ASC deficiency becomes a potential candidate for a causative mechanism of ALPS. Likewise, the treatment of this deficiency, which is still under development and aims at the reduction of the activation of caspase-1 and IL-1ß, also becomes a candidate treatment for ALPS.

ii. Another treatment, also under development, aims to reduce the excessive activity of the *NLRP3* Inflammasome. This reduction could be achieved through the *POP1* protein,

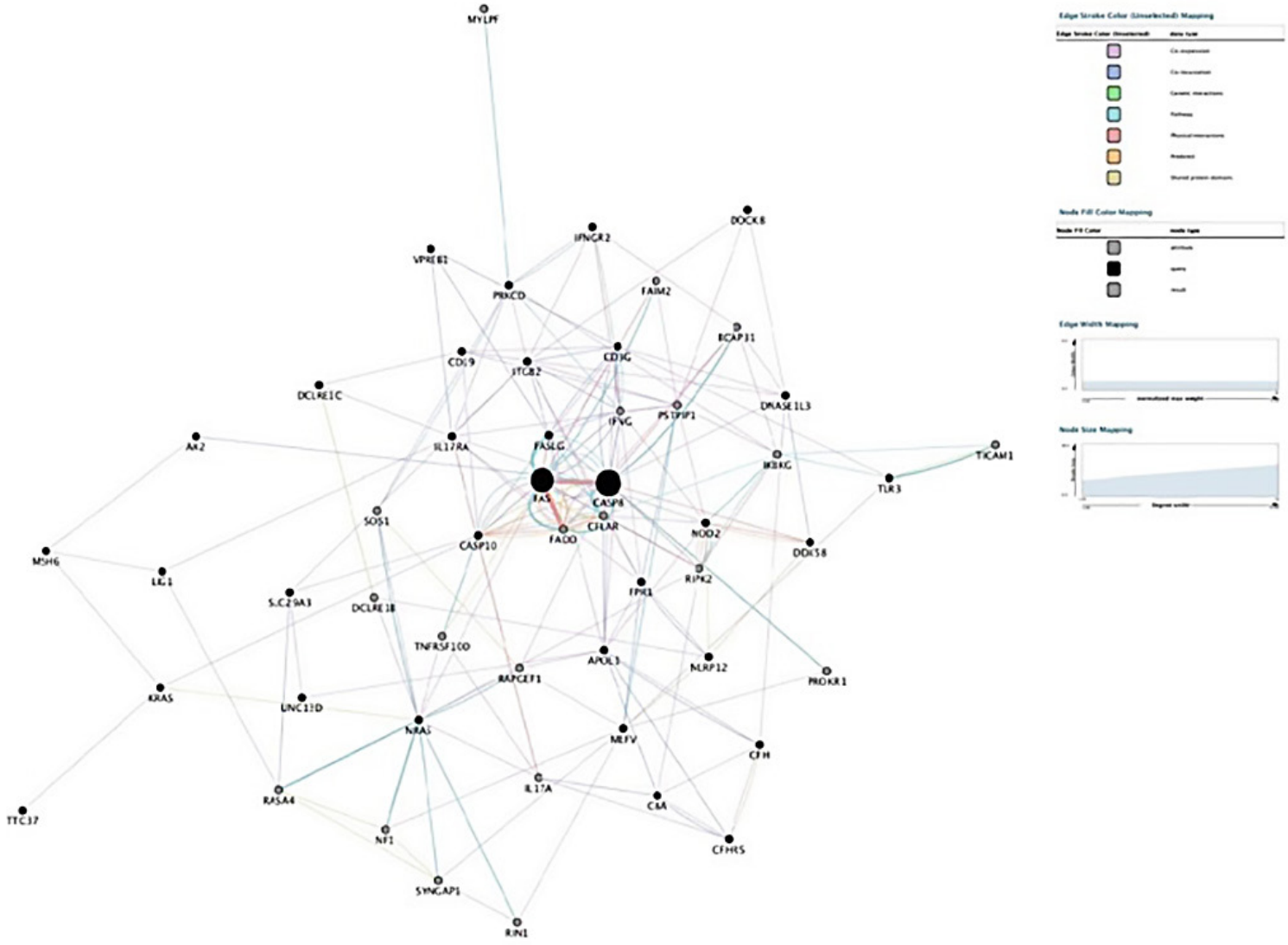

Figure 4. Network 3 generated by GeneMANIA® with information from CentiScaPe® through the Cytoscape® platform.

DOI: here
Reference here

capable of reducing the Inflammasome activity without inhibiting it.[12] This treatment is being developed for the *NLRP3*, a variation of the Inflammasome that is being studied by us; therefore, it has potential to be adapted to the *NLRP12*. There is still a need to develop effective treatments for ALPS with less severe side effects. The association found in this project with the *NLRP12* opens new treatment fronts for this extremely serious disease.

As previously discussed, some proteins that are highly intertwined with the body's innate immunity mechanisms appear with the same neighbors as proteins that are essential to cellular apoptosis. This fact reinforces the likelihood of a close relationship between innate immunity and cellular apoptosis—two major factors implicated in the risk of developing autoimmune diseases. As we improve our knowledge concerning the relationship between these two factors, we come closer to better understanding each one of them. Thus, understanding the relationship between innate immunity and cellular apoptosis might contribute to the knowledge concerning autoimmune diseases, and might improve the quality of life of at least 50 million people who suffer from autoimmune diseases worldwide (AARDA).

Experimental Methods. This project was developed using a systems biology approach, which examines the interaction between biological systems and their components in order to understand the function of certain molecules in their systems, and the function of certain systems in their organisms.

The main concepts of systems biology include: i) **network** – a group of elements that interact with each other by means of pair interactions; ii) **nodes** – the genes (proteins) connected with each other by edges; and iii) **edges** – known interactions between two elements. The distribution of interactions follows specific graph-theory laws, where most proteins have few interactions, and few proteins have hundreds of interactions. Another important characteristic of biological networks is their high level of clustering. Clusters are groups of genes that have common biological function and are more connected to each other than to other genes of the network.

In order to understand the function of an individual node, it is essential to use tools for visualization and analysis of the network's topological parameters. These tools include clustering [13] and network centralities. [14] Centralities are topological parameters that identify nodes with relevant positions in the network's global architecture.

First, we selected the genes for analysis in different computing platforms. This selection was made in several ways. ALPS genes were selected based on information from the US National Library of Medicine National Institute of Health – PUBMED. The list of genes implicated in the studied case in the first part of the investigation was compiled by the physicians involved in the patient's care. For the second part of the investigation, the genes were selected by the first author through direct observation of the exome sequencing data from the patient based on the following criteria: i) rare mutations; ii) non-synonymous mutations; iii) mutations located in regions of splicing sites; and iv) mutations predicted as deleterious to the proteins' functions in at least one of the databases. We used the following databases: *ExAC6500* [15], *PolyPhen-2* [16], *SIFT* [17], and *LRT*.[18] Thus, we made a second list including the genes with mutations considered deleterious.

The lists of selected genes were analyzed by four computing platforms: GeneMANIA®, Ingenuity®, LEGO® and Cytoscape®. The first three platforms were used in the first part of the investigation and the fourth was used in the second part of the investigation.

We will now present the different platforms used in this project. The utilization of more than one database ensured the validity of the results, as each platform uses a different database and has specific and novel criteria for gene selection, interactions, and biological pathways.

6-1 GeneMANIA®. [19] The platform GeneMANIA® (http://www.genemania.org) is a web interface that can generate hypotheses about gene functions, analyze gene lists and prioritize them by functions. Given a gene list, the platform presents their interactions and predicts new genes with similar functions using the genomics and proteomics data available. The program identifies the genes with the largest number of interactions in a group of genes using an extensive database with information about networks of functional interaction of many organisms. [19] GeneMANIA® uses public data including *co-expression data from Gene Expression Omnibus* (GEO) (1); *physical and genetic interaction data from BioGRID* (2); *predicted protein interaction data based on orthology from I2D* (3); *pathway and molecular interaction data from Pathway Commons, which contains data from BioGRID*; Memorial Sloan-Kettering Cancer Center, Human Protein Reference Database (4), *HumanCyc* (5), *Systems Biology Center New York, IntAct* (6), MINT (7), *NCI-Nature Pathway Interaction Database* (8) and *Reactome* (9). The platform also uses the Fischer's exact test; the P-value, which is the significance value that indicates the probability of the existence of an over-represented biological pathway associated with the genes that are being tested; and a multiple test comparison correction known as FDR (*Benjamini-Hochberg*).

6-2 Ingenuity®. Ingenuity® database utilizes an algorithm that identifies the relationship between genes, the regulation of cellular processes, cellular mechanisms, and functions. Ingenuity® is made up of many modules. For this study, we selected the canonical analysis module for biological processes (IPA).

We identified the most significant biological pathways of IPA database for the gene list. The level of significance between genes and biological pathways was measured in three different ways: i) through the division of the total number of genes related to a certain pathway (according to IPA database) by the number of genes in the network related to this pathway; ii) using Fischer's exact test; and iii) through the FDR test.

6-3 Lego ® [20]. LEGO® (Functional Link Enrichment of Gene Ontology or gene sets) is an algorithm that considers not only the biological pathway over-representation analysis (ORA) of a group of genes, but also the protein-protein interactions within this group to prioritize the genes and the over-represented biological pathways.

The algorithm puts together both analyses (biological pathways and interactions between genes) to carry out a more complete analysis. LEGO® uses the MsigDB (molecular signatures database (http://www.broadinstitute.org/gsea/msigdb/index.jsp.), which is composed of 7 other extensive databases: chemical and genetic disorders, canonical processes (*Biocarta gene sets*, *KEGG gene sets, Reactome gene sets*), gene expression regulators (*microRNA targets, transcription factor targets*), computational gene list (*cancer gene, cancer module*s), gene ontology (BP, MF, CC), cancer, and immunologic-related processes. The program also uses Fischer's exact test and the FDR test.

6-4 Cytoscape ® [21]. Cytoscape® is a free access platform used to visualize molecular interaction pathways and biological pathways, and to put these networks together with notes, gene expression profiles and other data. Through the platform, it is possible to use many different apps, developed by different institutions. Among those apps, we used:

6-4-1 GeneMania®. GeneMANIA® was used as a web interface in the first part of the investigation, and as an app for the Cytoscape® platform in the second part.

6-4-2 CentiScaPe ® [22]. CentiScaPe® identifies the most important genes in a protein-protein interaction network by calculating topologic parameters for each gene (protein). Here are some important concepts of the analysis through CentiScaPe®: i) the interaction between two nodes (genes) is always the shortest path between them; and ii) the higher a node's value, the closer it is to other nodes.

Although the app uses many different parameters to prioritize the nodes of a network, in this part of the study we used the three specific parameters that were considered to be the most relevant for the prioritization of nodes associated with complex diseases. [23, 24] We used the following parameters:

iii. Degree: an index that corresponds to the number of nodes adjacent to a node, i.e., the number of connections of a certain node.

iv. Betweenness: the amount of connections between pairs of nodes that pass through a certain node, which means that a node with a high *betweenness* is crucial to maintaining many interactions between pairs of nodes in a network. Genes with high *betweenness* are called *bottleneck* genes.

v. Bridging: the *bridging* value corresponds to the product of the *bridging coefficient* and the *betweenness centrality*, which means that a node with high *bridging* has highly connected first neighbors and at the same time is crucial to maintaining many connections between pairs of nodes. Genes with high *bridging* usually have few interactions, yet extremely significant ones.

6-4-3 MCode®. MCode® divides the genes of a network into clusters based on topology, to identify highly connected regions, usually implicated in the same cellular function.

Acknowledgements. The completion of this project would not have been possible without my advisor Dr. Carolina Cappi. I also want to thank Dr. Eduardo Finger for providing us with information about the medical case central to this project. Finally, I am grateful to the Department of Psychiatry, University of Sao Paulo Medical School for providing me with the space and resources needed to execute my research project.

References.

1. Hariri, B. M.; Cohen, N. A., New insights into upper airway innate immunity. *Am J Rhinol Allergy* **2016**, *30* (5), 319-23.

2. Janeway, C. A., Jr.; Medzhitov, R., Innate immune recognition. *Annu Rev Immunol* **2002**, *20*, 197-216.

3. Liston, A.; Masters, S. L., Homeostasis-altering molecular processes as mechanisms of inflammasome activation. *Nat Rev Immunol* **2017**, *17* (3), 208-214.

4. Vajjhala, P. R.; Lu, A.; Brown, D. L.; Pang, S. W.; Sagulenko, V.; Sester, D. P.; Cridland, S. O.; Hill, J. M.; Schroder, K.; Stow, J. L.; Wu, H.; Stacey, K. J., The Inflammasome Adaptor ASC Induces Procaspase-8 Death Effector Domain Filaments. *J Biol Chem* **2015**, *290* (49), 29217-30.

5. Cerwenka, A.; Lanier, L. L., Natural killer cell memory in infection, inflammation and cancer. *Nat Rev Immunol* **2016**, *16* (2), 112-23.

6. Azizi, G.; Pouyani, M. R.; Abolhassani, H.; Sharifi, L.; Dizaji, M. Z.; Mohammadi, J.; Mirshafiey, A.; Aghamohammadi, A., Cellular and molecular mechanisms of immune dysregulation and autoimmunity. *Cell Immunol* **2016**.

7. Barabási, A. L.; Gulbahce, N.; Loscalzo, J., Network Medicine: A Network-based Approach to Human Disease. *Nat Rev Genet* **2011**, *12* (1), 56-68.

8. Veto, B.; Bojcsuk, D.; Bacquet, C.; Kiss, J.; Sipeki, S.; Martin, L.; Buday, L.; Balint, B. L.; Aranyi, T., The transcriptional activity of hepatocyte nuclear factor 4 alpha is inhibited via phosphorylation by ERK1/2. *PLoS One* **2017**, *12* (2), e0172020.

9. Venugopal, P.; Koshy, T.; Lavu, V.; Ranga Rao, S.; Ramasamy, S.; Hariharan, S.; Venkatesan, V., Differential expression of microRNAs let-7a, miR-125b, miR-100, and miR-21 and interaction with NF-kB pathway genes in periodontitis pathogenesis. *Journal of cellular physiology* **2018**, *233* (8), 5877-5884.

10. Muro, Y.; Sugiura, K.; Mimori, T.; Akiyama, M., DNA mismatch repair enzymes: genetic defects and autoimmunity. *Clin Chim Acta* **2015**, *442*, 102-9.

11. Franklin, B. S.; Bossaller, L.; De Nardo, D.; Ratter, J. M.; Stutz, A.; Engels, G.; Brenker, C.; Nordhoff, M.; Mirandola, S. R.; Al-Amoudi, A.; Mangan, M. S.; Zimmer, S.; Monks, B. G.; Fricke, M.; Schmidt, R. E.; Espevik, T.; Jones, B.; Jarnicki, A. G.; Hansbro, P. M.; Busto, P.; Marshak-Rothstein, A.; Hornemann, S.; Aguzzi, A.; Kastenmuller, W.; Latz, E., The adaptor ASC has extracellular and 'prionoid' activities that propagate inflammation. *Nat Immunol* **2014**, *15* (8), 727-37.

12. de Almeida, L.; Khare, S.; Misharin, A. V.; Patel, R.; Ratsimandresey, R. A.; Wallin, M. C.; Perlman, H.; Greaves, D. R.; Hoffman, H. M.; Dorfleutner, A.; Stehlik, C., The PYRIN Domain-only Protein POP1 Inhibits Inflammasome Assembly and Ameliorates Inflammatory Disease. *Immunity* **2015**, *43* (2), 264-76.

13. Holme, P.; Huss, M.; Jeong, H., Subnetwork hierarchies of biochemical pathways. *Bioinformatics* **2003**, *19* (4), 532-8.

14. Wuchty, S.; Stadler, P. F., Centers of complex networks. *J Theor Biol* **2003**, *223* (1), 45-53.

15. Lek, M.; Karczewski, K. J.; Minikel, E. V.; Samocha, K. E.; Banks, E.; Fennell, T.; O'Donnell-Luria, A. H.; Ware, J. S.; Hill, A. J.; Cummings, B. B.; Tukiainen, T.; Birnbaum, D. P.; Kosmicki, J. A.; Duncan, L. E.; Estrada, K.; Zhao, F.; Zou, J.; Pierce-Hoffman, E.; Berghout, J.; Cooper, D. N.; Deflaux, N.; DePristo, M.; Do, R.; Flannick, J.; Fromer, M.; Gauthier, L.; Goldstein, J.; Gupta, N.; Howrigan, D.; Kiezun, A.; Kurki, M. I.; Moonshine, A. L.; Natarajan, P.; Orozco, L.; Peloso, G. M.; Poplin, R.; Rivas, M. A.; Ruano-Rubio, V.; Rose, S. A.; Ruderfer, D. M.; Shakir, K.; Stenson, P. D.; Stevens, C.; Thomas, B. P.; Tiao, G.; Tusie-Luna, M. T.; Weisburd, B.; Won, H.-H.; Yu, D.; Altshuler, D. M.; Ardissino, D.; Boehnke, M.; Danesh, J.; Donnelly, S.; Elosua, R.; Florez, J. C.; Gabriel, S. B.; Getz, G.; Glatt, S. J.; Hultman, C. M.; Kathiresan, S.; Laakso, M.; McCarroll, S.; McCarthy, M. I.; McGovern, D.; McPherson, R.; Neale, B. M.; Palotie, A.; Purcell, S. M.; Saleheen, D.; Scharf, J. M.; Sklar, P.; Sullivan, P. F.; Tuomilehto, J.; Tsuang, M. T.; Watkins, H. C.; Wilson, J. G.; Daly, M. J.; MacArthur, D. G.; Consortium, E. A., Analysis of protein-coding genetic variation in 60,706 humans. *Nature* **2016**, *536*, 285-291.

16. Adzhubei, I. A.; Schmidt, S.; Peshkin, L.; Ramensky, V. E.; Gerasimova, A.; Bork, P.; Kondrashov, A. S.; Sunyaev, S. R., A method and server

DOI: here
Reference here

for predicting damaging missense mutations. In *Nat Methods*, United States, 2010; Vol. 7, pp 248-9.

17. Ng, P. C.; Henikoff, S., SIFT: predicting amino acid changes that affect protein function. In *Nucleic Acids Res*, 2003; Vol. 31, pp 3812-4.

18. Liu, X.; Wu, C.; Li, C.; Boerwinkle, E., dbNSFP v3.0: A One-Stop Database of Functional Predictions and Annotations for Human Nonsynonymous and Splice-Site SNVs. *Hum Mutat* **2016**, *37* (3), 235-41.

19. Warde-Farley, D.; Donaldson, S. L.; Comes, O.; Zuberi, K.; Badrawi, R.; Chao, P.; Franz, M.; Grouios, C.; Kazi, F.; Lopes, C. T.; Maitland, A.; Mostafavi, S.; Montojo, J.; Shao, Q.; Wright, G.; Bader, G. D.; Morris, Q., The GeneMANIA prediction server: biological network integration for gene prioritization and predicting gene function. *Nucleic Acids Res* **2010**, *38* (Web Server issue), W214-20.

20. Dong, X.; Hao, Y.; Wang, X.; Tian, W., LEGO: a novel method for gene set over-representation analysis by incorporating network-based gene weights. *Sci Rep* **2016**, *6*, 18871.

21. Shannon, P.; Markiel, A.; Ozier, O.; Baliga, N. S.; Wang, J. T.; Ramage, D.; Amin, N.; Schwikowski, B.; Ideker, T., Cytoscape: a software environment for integrated models of biomolecular interaction networks. *Genome Res* **2003**, *13* (11), 2498-504.

22. Scardoni, G.; Tosadori, G.; Faizan, M.; Spoto, F.; Fabbri, F.; Laudanna, C., Biological network analysis with CentiScaPe: centralities and experimental dataset integration. *F1000Res* **2014**, *3*.

23. Yu, H.; Kim, P. M.; Sprecher, E.; Trifonov, V.; Gerstein, M., The importance of bottlenecks in protein networks: correlation with gene essentiality and expression dynamics. *PLoS Comput Biol* **2007**, *3* (4), e59.

24. Liu, Y. Y.; Slotine, J. J.; Barabasi, A. L., Control centrality and hierarchical structure in complex networks. *PLoS One* **2012**, *7* (9), e44459.

Appendices.

Symbol	Name	Location
CASP10	caspase 10	Cytoplasm
CASP8	caspase 8	Nucleus
FAS	Fas cell surface death receptor	Plasma membrane
FASLG	Fas ligand	Extracellular space
KRAS	Kirsten rat sarcoma viral oncogene homolog	Cytoplasm
NRAS	neruoblastoma RAS viral oncogene homolog	Plasma membrane
PRKCD	protein kinase C delta	Cytoplasm

Appendix A. Genes that have previously been implicated in ALPS (seed genes in network 2) - list generated by Ingenuity®.

Symbol	Name	Location	Type
AK2	adenylate kinase 2	Cytoplasm	kinase
APOL1	apolipoprotein L1	Extracellular Space	transporter
C8A	complement C8 alpha chain	Extracellular Space	other
CASP10	caspase 10	Cytoplasm	peptidase
CD19	CD19 molecule	Plasma Membrane	transmembrane receptor
CD3G	CD3g molecule	Plasma Membrane	transmembrane receptor
CFH	complement factor H	Extracellular Space	other
CFHR5	complement factor H related 5	Extracellular Space	other
DCLRE1C	DNA cross-link repair 1C	Nucleus	enzyme
DDX58	DExD/H-box helicase 58	Cytoplasm	enzyme
DNASE1L3	deoxyribonuclease 1 like 3	Nucleus	enzyme
DOCK8	dedicator of cytokinesis 8	Cytoplasm	other
FPR1	formyl peptide receptor 1	Plasma Membrane	G-protein coupled receptor
IFNGR2	interferon gamma receptor 2 (interferon gamma transducer 1)	Plasma Membrane	transmembrane receptor
IL17RA	interleukin 17 receptor A	Plasma Membrane	transmembrane receptor
ITGB2	integrin subunit beta 2	Plasma Membrane	transmembrane receptor
LIG1	DNA ligase 1	Nucleus	enzyme
MEFV	MEFV, pyrin innate immunity regulator	Nucleus	other
MSH6	mutS homolog 6	Nucleus	enzyme
NLRP12	NLR family pyrin domain containing 12	Cytoplasm	other
NOD2	nucleotide binding oligomerization domain containing 2	Cytoplasm	other
SLC29A3	solute carrier family 29 member 3	Plasma Membrane	transporter
TLR3	toll like receptor 3	Plasma Membrane	transmembrane receptor
TTC37	tetratricopeptide repeat domain 37	Nucleus	other
UNC13D	unc-13 homolog D	Cytoplasm	other
VPREB1	pre-B lymphocyte 1	Plasma Membrane	other

Appendix B. Genes possibly implicated in the reported case (seed genes in network 1) - list generated by Ingenuity®.

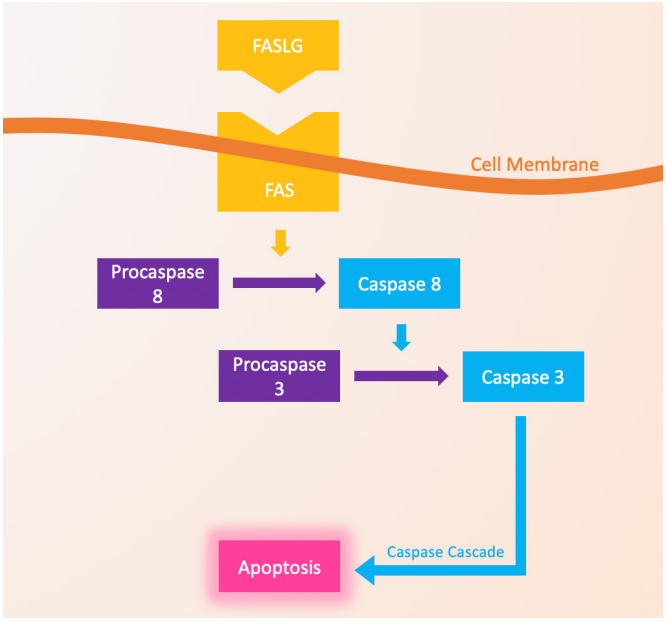

Appendix C. Extrinsic apoptosis signaling pathway.

Authors. I am a sophomore at Scheck Hillel Community School. I was born in Sao Paulo, Brazil, and moved to Miami, Florida in April of 2017. I am highly interested in pursuing a research-based science career with a focus on immunology and medicine.

Fibers from grape leaves: thermo-gravimetric and differential scanning calorimetry analysis

Obada Nayef Al-leimon*, Ahmad Nayef Al-leimon

King Abdullah II School for Excellence, Al Marj, Al karak, 61112, Jordan

*obada-nayef@outlook.com

ABSTRACT: We prepared fibers from an alternative source, dry grape leaves, using a simple and low-cost procedure. The thermal analysis of the prepared fibers obtained from dry grape leaves using thermal gravimetric analysis (TGA) and differential scanning calorimetry (DSC) shows similar characteristics to that of standard cotton. Furthermore, chemical analysis of the remaining grape leaves' biomass after cotton fiber preparation indicated its potential use as biofertilizer.

KEYWORDS: Agro-waste; Grape leaves; Cotton fibers; TGA; DSCA; Biofertilizer

Introduction. Agro-waste is defined as waste that is produced from various agriculture activities that includes different parts of plants that are usually considered useless and are ultimately discarded.[1] The agro-waste of grape farms and related industries includes grape leaves and the pomace. Several reports have documented the beneficial use of grape waste produced from wine and juice production. During wine production, approximately 25% of the grape weight results in by-product/waste, termed 'pomace', which is comprised of skins and seeds.[2] Various applications for grape pomace have been reported including functional food production, biosurfactants, cosmetics, pharmaceuticals, supplements, gold nanoparticles, dye removal and as an effective adsorbent for Cr(VI).[2,3,4,5,6] Meanwhile, very limited work has been done to investigate the potential use of the other components of grape farm waste including grape leaves.

Deciduous plants are those plants that lose their leaves at certain times of the year in a process called abscission. These plants include trees, perennial herbs, and shrubs. Huge quantities of leaf biomass fall to the ground every year and help to recycle natural carbon, nitrogen, phosphorous, sulfur and several other mineral nutrients of the soil when decayed. Plant leaves contain many derivatives of the four major biological molecules in their cellular structure. Among the four major biological molecules, the derivatives of polysaccharides called cellulose are considered the most abundant biological molecule on earth.

Cotton produced by plants of the genus Gossypium is produced as a seed hair or white fibrous pulp composed largely of cellulose and other non-cellulosic materials. Cellulose is a complex molecule of glucose polymers linked by glycosidic covalent bonds. It has very important mechanical and physical properties that lead to greater resistance to chemical effects when compared with other polysaccharides. Cotton is considered the most important fibrous material used in the textile industry. However, due to shortages in cotton production and many other economical and agricultural reasons, the industry began to replace cotton with crude oil derivatives and polymers.[7] Recently, the fluctuating and increasing crude oil prices, political issues, and oil shortages related to their unrenewable nature has led researchers to find other alternatives that are ecofriendly, renewable, as well as degradable to substitute for crude oil textile polymers and the shortage in the natural cotton supplies., The folk application of fallen grape leaves, treated or untreated, as bio-fertilizer is already known, while other applications have been rarely reported. Therefore, the aims of this project were to recycle fallen grape leaves and to evaluate their potential as a source of cotton fiber using a simple and cheap approach. Furthermore, we will evaluate grape biomass as a soil amendment to support the growth of plants.

These include functional foods, biosurfactants, cosmetics, pharmaceuticals, supplements, production of gold nanoparticles, adsorbent for Cr(VI) and dye removal. [2,3,4,5] The potential of grape leaves as agro-waste has been poorly studied. In 2013 and 2016, respectively reported grape leaves as a rich source of phenolics compounds and resveratrol as an important stilbene that benefits human health.8,9 However, the idea of extracting cellulosic fibers and cotton fibers from the dry grape leaves was never reported.

Results and Discussion. Cotton fibers from fallen grape leaves were successfully prepared through a simple and cheap procedure as illustrated in the experimental methodology. Figure 1 shows the biomass of the prepared white cotton fibers from dry grape leaves. However, the utilization of grape winery waste known as pomace (grape waste comprised of skins and seeds) in a vast array of applications has been previously reported. [2]

The resulting cotton fibers obtained from the dry grape leaves were further characterized and compared with normal cotton using thermal gravimetric analysis (TGA) and differential scanning calorimetry (DSC). The results of thermal analysis appear in Figure 2 and 3 as a comparison between grape cotton

DOI: here
Reference here

(Figure 2) and natural cotton (Figure 3) and shows that they have the same characteristics.

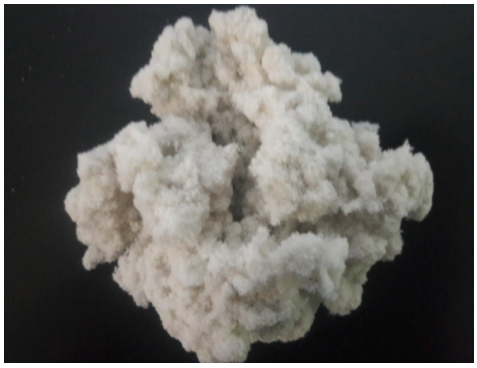

Figure 1. White biomass of cotton fibers prepared from dry grape leaves.

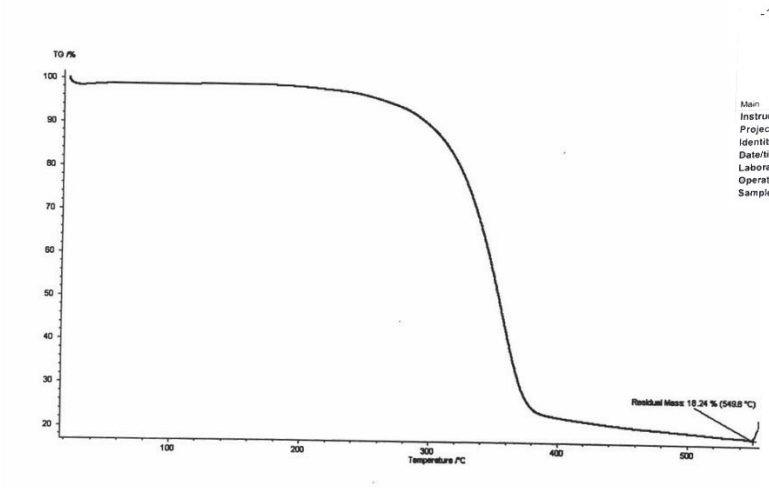

Figure 2. TGA analysis of grape cotton.

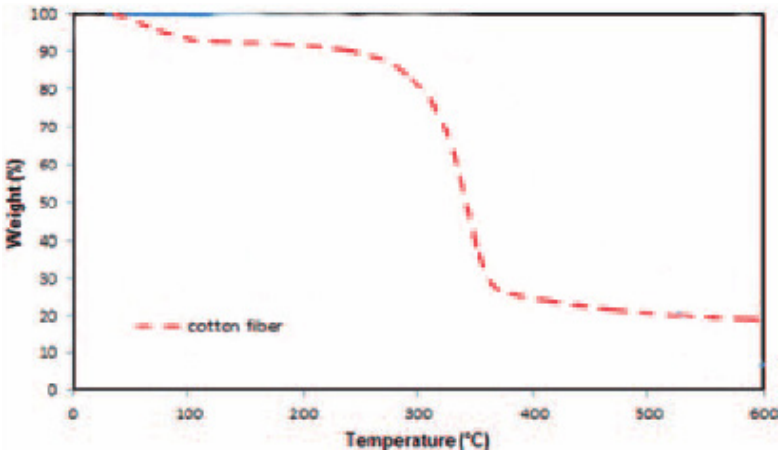

Figure 3. TGA Analysis of natural cotton.

Differential scanning calorimetry, or DSC, is a thermos-analytical technique in which the difference in the amount of heat required to increase the temperature of a sample and a reference is measured as a function of temperature. When test grape cotton was compared with normal cotton using differential scanning calorimetry, or DSC, the results (Figure 4) showed that, the sample (grape cotton) and the reference (standard cotton) were maintained at nearly the same temperature throughout the experiment. As a result, our product (grape cotton) as analyzed by TGA and DSC tests appears to have the same physical and chemical properties.

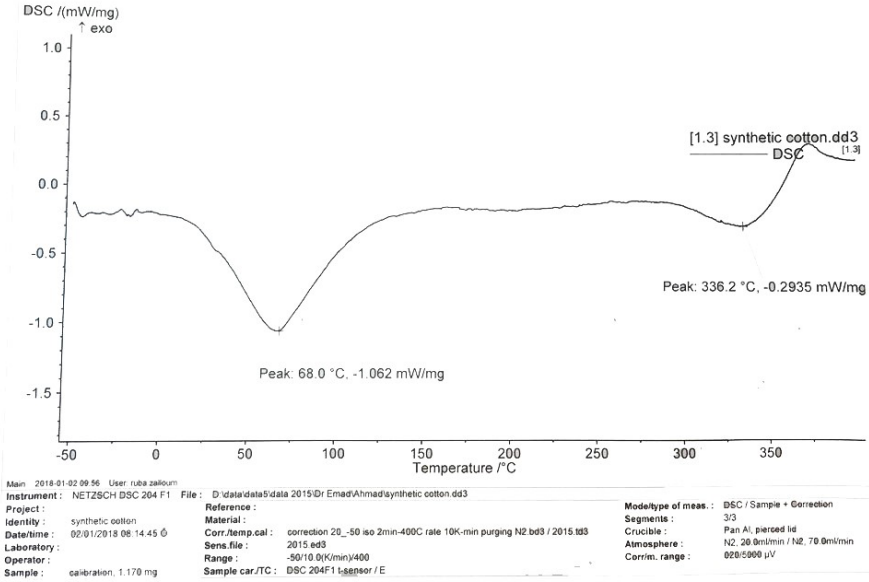

Figure 4. (DSC) - For grapes cotton.

Furthermore, the resulting biomass after grape cotton preparation as well as the huge biomass of the fallen grape leaves seems to be interesting agro-waste product. The chemical analysis shown in Table 1 indicated the usefulness of the remaining biomass of the dry grape (Figure 5) leaves after fiber preparation as potential fertilizer. The chemical analysis results showed that several mineral salts as well as potassium, phosphorus and nitrogen are present in considerable amounts. The presence of such nutritional minerals in grape leaves makes them a potential organic ecofriendly amendment to the soil to support the growth of several cultivated crops.

Figure 5. Grape leaves material remaining after fiber preparation.

Experimental Methods. The fallen grape leaves were collected in the months of October and November. Grape cotton was prepared as follows: approximately 200 g of dry grape leaves were collected and ground using an electrical grinder. The ground grape leaf biomass was then sieved using a soft strainer to separate the fibers from the rest of biomass. A total

of 100 mL sodium hypochlorite (6% - 6.25%) were added to the fibers prepared from the dry grape leaves. The fibers were washed two times with 200 mL water to remove the sodium hypochlorite. Finally, samples of the washed cotton fibers prepared from the grape leaves were subjected to thermal gravimetric analysis (TGA) and differential scanning calorimetry (DSC). The TGA and DSC analyses were performed in the laboratories of the National Center for Agricultural Research and Extension (NCARE), Alraba, Jordan. In addition, the remaining grape leaves biomass after fiber preparation was evaluated as a potential organic fertilizer through an NPK and other minerals analyses. The NPK analysis was performed in the laboratories of the National Center for Agricultural Research and Extension (NCARE), Alraba, Jordan.[10]

P	K	N	Ca	Mg
%	%	%	%	%
0.122	0.50	1.39	5.61	0.59
Mn	Zn	Cu	Fe	
Ppm	Ppm	Ppm	Ppm	
123	19.7	13.8	1534	

Table 1. Chemical composition of the remaining biomass from grape leaves.

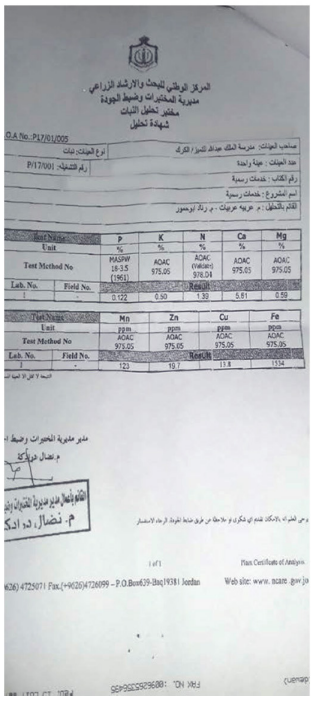

Figure 6. Chemical composition certificate obtained from NCARE

TGA is a thermal analysis method in which the mass of a sample is measured over time as the temperature changes. This measurement provides information about physical phenomena, such as phase transitions, absorption and desorption; as well as chemical phenomena including chemisorption, thermal decomposition, and oxidation or reduction.

Conclusion. The present work reported the use of the dry grape leaves as a source of cotton fibers and as organic fertilizer. The results revealed that the thermal characteristics of the prepared grape leaf cotton was similar to the thermal properties of the standard cotton. In addition, the chemical composition of the leftover grape leaf biomass after preparation of cotton fibers can be used as an ecofriendly fertilizer to support the growth and production of cultivated crops as well as be used for filtration, production of different textiles, and for natural industries.

Acknowledgement. The researchers acknowledge the National Center for Agricultural Research and Extension (NCARE), Alraba, Jordan as well as the Chemistry labs in the University of Jordan for conducting the analytical experiment.

References.

1. Lim, S. F., & Matu, S. U. (2015). Utilization of agro-wastes to produce biofertilizer. International Journal of Energy and Environmental Engineering, 6(1), 31-35.

2. Dwyer, K., Hosseinian, F., & Rod, M. (2014). The market potential of grape waste alternatives. Journal of Food Research, 3(2), 91-106.

3. Krishnaswamy, K., Vali, H., & Orsat, V. (2014). Value-adding to grape waste: Green synthesis of gold nanoparticles. Journal of Food Engineering, 142, 210-220.

4. Chand, R., Narimura, K., Kawakita, H., Ohto, K., Watari, T., & Inoue, K. (2009). Grape waste as a biosorbent for removing Cr (VI) from aqueous solution. Journal of Hazardous Materials, 163(1), 245-250.

5. Sayğılı, H., Güzel, F., & Önal, Y. (2015). Conversion of grape industrial processing waste to activated carbon sorbent and its performance in cationic and anionic dyes adsorption. Journal of Cleaner Production, 93, 84-93.

6. Barros, A., Gironés-Vilaplana, A., **Teixeira**, A., Collado-González, J., Moreno, D. A., Gil-Izquierdo, A., ... & Domínguez-Perles, R. (2014). Evaluation of grape (Vitis vinifera L.) stems from Portuguese varieties as a resource of (poly) phenolic compounds: A comparative study. Food Research International, 65, 375-384.

7. Course of organic chemistry, dr.pafloof (курс органической химии)From page 390 to 400 – about Cellulose.

8. Wang, L., Xu, M., Liu, C., Wang, J., Xi, H., Wu, B., ... & Li, S. (2013). Resveratrols in grape berry skins and leaves in Vitis germplasm. PloS one, 8(4), e61642.

9. Chakraborty, P., Joseph, J. S., Naushad, T., & Abraham, J. (2016). Cytotoxicity and bioactivity of grape leaves extracts. International Journal of Pharma and Bio Sciences, 7.

10. Page, A. L.(ed). 1982. Methods of soil analysis, 9, Part 2: Chemical and mineralogical properties,2nd ed., Am. Soc, Madison, WI, USA.

DOI: here
Reference here

Less light, more growth? Effects of the abscemce of light on roots of *in vitro* of *Catasetum fimbriatum* (Orchidaceae)

Regina A. Amadeu

Colégio Dante Alighieri, Al. Jaú 1061, São Paulo, SP, CEP 01420-003, Brazil

regina.amadeu@colegiodante.com.br

ABSTRACT: Due to the beauty of their flowers, orchids are extremely valued and commercialized. However, under natural conditions, the chances of reproduction are low. Thus, *in vitro* cultivation becomes an excellent option for rapid proliferation and for obtaining numerous plants with high genetic and phytosanitary quality. Among the many factors utilized to increase the efficiency and speed of production of these plants is the addition of activated carbon, which has been used due to its positive influence on the height and rooting in some species. The objective of this work was to find a way to improve the *in vitro* development of *Catasetum fimbriatum* in a simpler and cheaper way, without the use of activated carbon. My hypothesis is that the effect of light deprivation on the roots of the orchid could result in a development equivalent to that of the plant whose culture medium has activated charcoal, since I believe the growth of the orchid is not helped by the charcoal itself, but by the darkness it provides to the plant. Specimens of *Catasetum fimbriatum* were used as study material. The plants were studied in three groups, the first one (control) in conventional culture medium, the second with addition of activated carbon and the third with light deprivation in orchid roots. After three months, the specimens were evaluated according to the largest length of the root, length of the largest leaf, shoot fresh mass and root fresh weight. I found significant variations ($p < 0.05$) in the different groups, and the one with greatest relevance (statistical significance) was the length of the largest root between group 1 (activated charcoal) and 2 (deprivation of light), which showed longer roots. We can conclude that light deprivation would be a good alternative to activated charcoal, since a longer root length may favor the rooting of the plant when transferred to the growth vessel, although the root length of the plant may also depend on the presence of phenols. Other studies should be performed to clarify the nutritional influence of activated carbon on the *in vitro* culture of *Catasetum fimbriatum.*

KEYWORDS: Orchids; *Catasetum fimbriatum;* Activated charcoal; *In vitro* culture

Introduction. Due to the beauty of its flowers, plants of the Orchidaceae family are extremely valued and commercialized. Orchidaceae comprises about 7% of all angiosperms, being considered one of the largest families of this group and presenting about 850 genera and 20,000 species distributed throughout the world. Moreover, its greatest diversity is found in the tropics. In Brazil alone, there are about 2,300 species distributed in 191 genera.[1]

Among these genera, *Catasetum*, from the subfamily Epidendroideae,[2] stands out due to its sexual dimorphism and a complex mechanism for pollination.[3] They are distributed throughout the Americas, especially in the tropical zone. The species *Catasetum fimbriatum* occurs only in South America, mainly in Brazil, Bolivia, Venezuela, and Argentina.[4]

Given the economic potential in their exploration, orchids have been extricated from their natural habitats. In addition, the advancement of agriculture has altered the ecosystems where they occur, further hindering their survival and reproduction.

Under natural conditions, many angiosperms depend on the dissemination of seeds and require the association with mycorrhizal fungi for germination, consequently decreasing chances of success in multiplication.[5] Thus, *in vitro* techniques have proven to be a reasonable alternative for the propagation of orchids, since the plants stop depending on the presence of fungi and exhibit faster proliferation, making it possible to obtain a large number of plants with a high genetic and phytosanitary quality.[6]

In vitro culture demands, for different species of Orchidaceae, specific culture media often modified with complex additives in order to provide the most favorable conditions of growth.[7,8] Activated charcoal is traditionally exploited to increase the efficiency and growth speed of *in vitro* cultures.[9] The use of charcoal may be beneficial to *in vitro* cultures of orchids due to its influence on the height and rooting of some species.[5,10]

However, the real cause of the benefits of the addition of charcoal to the culture medium remains unclear. Such effects have been attributed to the formation of a dark environment in the medium or to the adsorption of substances such as phenols, ethylene, growth regulators, vitamins and other organic compounds.[11]

According to Pan and Staden[11], a problem frequently encountered during the early stages of *in vitro* culture is the eventual tissue death due to excessive production of polyphenols, possibly triggering defense reactions. Polyphenols often

DOI: here
Reference here

have the connotation as being inhibitory substances that should be avoided or eliminated from *in vitro* environments. Although there are several methods of preventing the accumulation of such compounds, incorporation of charcoal or polyvinylpyrrolidone into crops can prevent phenolic adsorption and render polyphenol oxidase and peroxidase inactive.[11]

Auxins and cytokinins are plant growth regulators frequently used in *in vitro* cultures, and their concentrations and combinations in the culture medium is generally an important factor that determines successful plant regeneration. The use of activated charcoal for the adsorption of toxic plant metabolites is known. Activated charcoal is able to adsorb high concentrations of some growth regulators in liquid and solid media.[10]

Pan and Staden[11] also suggest that it is possible for activated charcoal to excrete growth promoting substances, but they do point out that it requires more studies

According to Moraes and colleages[12], activated charcoal has been used to stimulate rooting because of its high capacity to exclude light from the culture medium and to reduce crop oxidation by the presence of phenols produced by the tissues themselves.

In addition, according to the theory of positive and negative phototropism, the aerial part of the plant grows toward the light and the root develops in the opposite direction. Therefore, the objective of the study was to verify if the effect of light deprivation on the *in vitro* culture of *Catasetum fimbriatum* could result in an equivalent development to that of plants growing on culture medium with activated charcoal. Accordingly, we believed the factor that would aid in orchid growth would not be the charcoal itself, but the darkness it provides to the plant.

Results and Discussion. After three months of *in vitro* culture, all the plants were analyzed (Fig. 4) and the measurements were taken (Table 1).

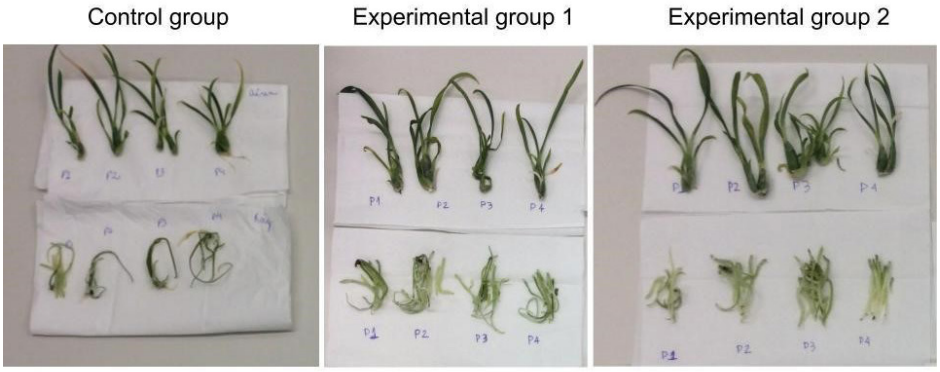

Figure 4. Examples of some individuals for three groups of plants after growth. The shoots and the roots for each plant were detached to proceed with the measurements.

The mean of the shoot fresh mass of the control group was significantly smaller than that of the experimental group 1. The mean of the root fresh mass of the experimental group 2 was significantly heavier than that of the control group, although experimental group 2 showed significantly longer root length mean compared to experimental group 1 (Table 2).

Groups	Shoot fresh mass (g)	Root fresh mass (g)	Largest leaf length (cm)	Largest root length (cm)
Control	0.43±0.23	0.33±0.18	4.85±2.09	5.18±2.59
Experimental group 1	**0.76**±0.63	0.54±0.47	5.01±2.09	4.33±1.07
Experimental group 2	0.58±0.41	**0.55**±0.41	5.36±2.49	5.95±2.35

Table 1. Mean values for the largest leaf length, largest root length, shoot fresh weight and root fresh mass of* Catasetum fimbriatum *individuals after 112 days of cultivation, in the three experimental groups. Means in bold were significantly different (p<0,05) from means of the control group.

Groups	Shoot fresh mass	Root fresh mass	Largest leaf length	Largest root length
Control / Experimental 1	**0.03**	0.07	0.83	0.20
Control / Experimental 2	0.17	**0.04**	0.53	0.36
Experimental 1 / Experimental 2	0.36	0.97	0.52	**0.01**

Table 2. Results of the ANOVA for the means of the largest leaf length, largest root length, shoot fresh mass and root fresh mass of individuals in Catasetum fimbriatum (α=0.05).

Conclusion. Based on the observed results, we can conclude that, depending on the objective of the producers, light deprivation would be a good alternative as a substitute for activated charcoal, since a longer root length may favor the rooting of the plant when transferred to a vessel, although the root length of the plant may also depend on the presence of phenols. Despite all this, the presented information is useful to guide further studies on this subject.

Methods. The experiment was carried out at the Biotechnology Laboratory of the Dante Alighieri School (São Paulo, Brazil). The species used as study material was *Catasetum fimbriatum* (Orchidaceae).

The nodal segments of an etiolated plant were used for micropropagation and inoculated in 22 mm x 200 mm test tubes containing 20 mL of the culture medium Universidade de São Paulo (USP) (Fig. 1).[13] The culture medium pH was adjusted to 5.8 ± 0.1 before autoclaving.

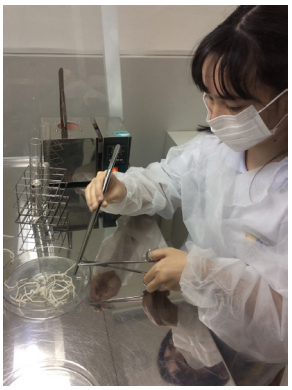

Figure 1. Nodal segments being inoculated in the culture medium by the author.

The specimens were separated into three experimental groups: control group with culture medium without activated charcoal in test tubes without any cover; experimental group

DOI: here
Reference here

1 with activated charcoal added to the culture medium (5.0 g/L) in test tubes without any cover; and experimental group 2, with culture medium without activated charcoal and test tube wrapped with aluminum foil at the bottom, in order to seal the plant root of light. A layer of pre-autoclaved black glass beads was added in all experimental groups to block light from above (Fig. 2).

Metodologia

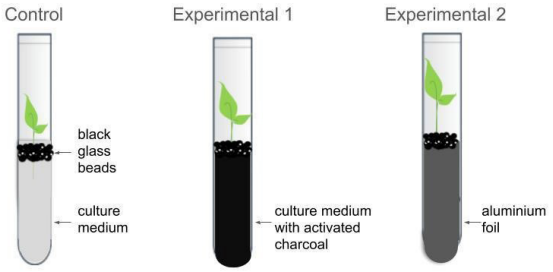

Figure 2. Scheme of test tubes for the three experimental groups.

Each experimental group consisted of 20 tubes with a nodal segment, totaling 60 individuals.

The test tubes were kept in a growth room for 112 days at a temperature of 22 ± 3 ˚C, photoperiod of 12 hours and a light intensity of 1300 lux. The analyzed variables were: root length, leaf length (one per plant), shoot fresh mass and roots fresh mass (Fig. 3).

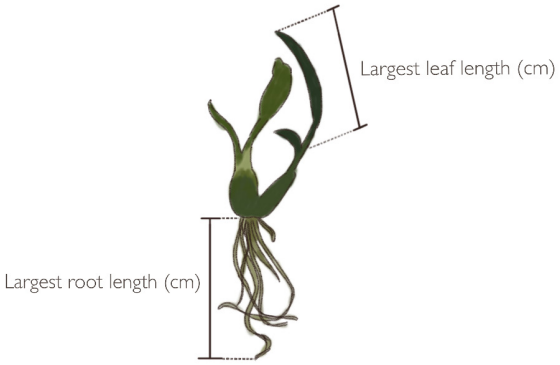

Figure 3. Illustration of how the measurements were taken.

The measurement means of each of the groups were compared in a one-way ANOVA test, with a significance level of 5%, after being submitted to the Doornik-Hansen normality test.

Acknowledgements. To my advisors Nilce de Angelo and Fernando C. de Domenico and to my co-advisor Sandra Maria R. Tonidandel. Also, I would like to thank all the team responsible for the Programa de Pré-iniciação Científica Cientista Aprendiz (a scientific pre-initiation program) of Dante Alighieri School for the valuable support.

References.

1. Barros, F. Diversidade taxonômica e distribuição geográfica das Orchidaceae brasileiras. Acta Bot. Bras. **1990**, *4*, 177-187

2. Machnicki-Reis, M.; Engels, M. E.; Petini-Benelli, A.; Smidt, E. C. O gênero *Catasetum* Rich. ex Kunth (Orchidaceae, Catasetinae) no Estado do Paraná, Brasil. *Hoehnea*, **2015**, *42*, 185-194.

3. Romero, G. A. Non-functional flowers in *Catasetum fimbriatum* orchids (Catasetinae, Orchidaceae). *Bot. J. Linn. Soc.* **1992**, *109*, 305-313.

4. Ferreira, A. W. C. 2005. Fenologia de *Catasetum fimbriatum* (Morren) Lindl. (Catasetinae, Orchidaceae) e sua polinização por abelhas Euglossini (Hymenoptera, Apidae) na região de São Carlos-SP, Brasil. M.Sc. Thesis, Universidade Federal de São Carlos, 2005.

5. Soares, J. S.; Rosa, Y. B. C. J.; Macedo, M. C.; Sorgato, J. C.; Rosa, D. B. C. J.; Rosa, C. B. C. J. Cultivo *in vitro* de *Brassavola tuberculata* (Orchidaceae) em meio de cultura alternativo suplementado com diferentes concentrações de açúcar e carvão ativado. Magistra **2012**, *24*, 226-233.

6. Figueiredo, M. A.; Pasqual, M.; Araujo, A. G.; Junqueira, K. P.; Santos, F. C.; Rodrigues, V. A. Fontes de potássio no crescimento *in vitro* de plantas de orquídea *Cattleya loddigesii. Ciênc. Rural* **2008**, *38*, 255-257.

7. Campos, D. M. *Orquídeas: reprodução por sementes em laboratório caseiro*; 2010.

8. Morales, S.; Mulaneze, M. A. G.; Machado, M. F. P. S. Effect of Activated Charcoal for Seedlings Development of *Catasetum fimbriatum* Lindl (Orchidaceae). *J. Plant Sci.* **2006**, *4*, 87-93.

9. Arditti, J.; Ernst, R. *Micropropagation of orchids*; J. Wiley: New York, 1993.

10. Prizao, E. C. Efeito de carvão ativado e do grafite no crescimento *in vitro* de orquídeas. M.Sc. Theses, Universidade Estadual de Maringá, 2007.

11. Pan, M. J.; Staden J. The use of charcoal in in vitro culture - A review. *Plant Growth Regul*. **1998**, *26*, 155-163.

12. Moraes, A. P.; Tacuatiá, L. O.; Carvalho, F. I. F.; Kalchuk-Santos. 2009. Androgênese em milho: cultura *in vitro* e desenvolvimento dos micrósporos em genótipos brasileiros. *Plant Cell Cult. Micropropag*. **2009**, *5*, 79-86.

13. Chaer, L. Estudo para o estabelecimento de uma nova estratégia de clonagem in vitro de *Cattleya e Cymbidium* (Orchidaceae) por meio da utilização de gemas laterais de caules estiolados. M.Sc. Thesis, Universidade de São Paulo, 2012.

Authors. I'm a 15- year-old scientist who has been conducting my own scientific studies since I was 12. At the present, I'm involved with a new study about Tourette syndrome.

Basalt as an alternative to limestone in the production of Portland cement

Sophia L. Shapiro

Avenues: New York, 455 W. 23rd St. Apt 17 AB, New York, 10011, USA

sshapiro19@avenues.org

ABSTRACT: A wide range of environmental consequences will occur due to anthropogenic climate change caused by carbon dioxide emissions.[1] Cement production accounts for 6% of these carbon emissions, releasing around 2.25 x 10^9 tons of carbon dioxide annually.[2] When limestone is heated, it emits CO_2 into the atmosphere through a process called calcination, due to the prevalence of calcium carbonate.[3] Scientists are aware of this problem, however there is no sign that the cement industry will change. Cement is the primary ingredient in concrete, and concrete is the second most consumed substance on Earth after water.[4] This paper proposes the use of basalt as the primary ingredient in the production of Portland cement. Through the synthesis of cement with basalt and following calculations, the following paper concluded that if limestone were substituted for basalt, 3.9375 x 10^8 metric tons of CO_2 would be saved. These findings support the thesis that using basalt as the primary ingredient in cement would be a viable comfortable conservation solution.

KEYWORDS: Climate change; Carbon dioxide; Cement; Basalt; Calcination; Hydration

Introduction. In 2014, global CO_2 emissions from industrial processes were around 37.5 x 10^9 tons; 2.25 x 10^9 tons of which were from cement production.5 Half of these emissions were due to the burning of fossil fuels, while the other half is accounted for by the calcination process.[6] During the calcination process, limestone used in cement is heated, and the carbon present in the rock is released and oxidized to form CO^2 and quicklime:

$$CaCO_3 \rightarrow CaO + CO_2$$

While there are some existing solutions to this problem, none of them are comfortable conservation solutions. The term "comfortable conservation" is used to classify a type of solution that accomplishes the set goal without disturbing daily life, oftentimes even improving it. The method most often discussed involves blending other materials with limestone to reduce emissions from the limestone itself. This technique is called blended cement. Blended cement involves replacing a percentage of the limestone primarily with fly ash. Fly ash is produced when coal is heated to temperatures as high as 2800 degrees Fahrenheit.[7] In this way, fossil fuels must be burned to produce the fly ash. This method, however, does cost less than normal Portland cement.

Portland cement costs vary from around $50 to $75 per ton, while fly ash prices range from $15 to $40 per ton.[8] Unlike Portland cement, a major portion of the cost of fly ash is in transportation, as is demonstrated by the increased cost for fly ash in remote locations. The use of fly ash, however, is probably not a solution to decreasing carbon emissions. This technology has been around for years, but because of the transportation and the decrease in strength of the cement, many companies prefer to use limestone.[9]

Basalt and Portland Cement Chemical Composition. Basalt is a fine grained, igneous rock composed mostly of plagioclase and pyroxene minerals. Plagioclase is a term used to classify a group of minerals that are homogeneous mixtures of albite and anorthite. In addition, basalt also contains high levels of magnesium, silica, and iron.[10] Unlike the limestone used in cement, there is no exact chemical formula for the composition of basalt.

Portland cement is essentially composed of crushed and heated limestone. Limestone is chemically represented as $CaCO_3$. Lime (CaO) is derived from the limestone, and oftentimes silica, iron, and magnesium are added depending on the desired strength and composition. Calcium oxide is the largest component of cement, accounting for an average of 63.81% of its composition.[11]

In order to significantly reduce the emissions from calcination, basalt would be an ideal replacement for carbon-emitting limestone. Components of basalt such as iron, magnesium, and silica are all normally found in cement, but the lack of calcium carbonate makes it an appropriate substitute. Since all of the essential components to cement are present in this one igneous rock, only a small percentage of lime would be needed. However, about 50% of basalt is silica, which is often added to Portland cement to strengthen the mixture.[12] Since there is a lack of calcium carbonate in basalt, no carbon dioxide can be produced from its heating. However, supplemental lime would be needed to strengthen the cement.

The Production of Portland Cement. The process of cement production, demonstrated in **figure 1** below, begins

DOI: here
Reference here

with the extraction of limestone. The proposed solution would start with basalt instead. Once the natural rocks or minerals are extracted, they are sent to a production facility where they are crushed through a milling process and stored in large chambers called silos. This fine powder, known as raw meal, is then preheated and sent to a kiln. The kiln is heated between 950-1500 degrees Celsius. Chemical reactions take place during the heating process to form cement clinker. After being processed at such high temperatures, the initial oxides (CaO, SiO_2, Al_2O_3, and Fe_2O_3), then present in the form of mineral oxides: alite ($3CaO{\bullet}SiO_2$, C_3S), belite ($2CaO{\bullet}SiO_2$, C_2S), celite ($3CaO{\bullet}Al_2O_3$, C_3A), and felite ($4CaO{\bullet}Al_2O{\bullet}Fe_2O_3$, C_4AF).[13] The kiln itself is angled at 3 degrees allowing the clinker to pass through. Upon exiting, the clinker is cooled and then ground again to produce cement. A small amount of gypsum is usually added, which determines how the cement will set.[14] Without the addition of gypsum, C_3A will react quickly with water, resulting in the flash setting of concrete. Finally, the cement is packaged and transported to the desired locations.[15]

Hydration. These reactions are exothermic, and therefore generate heat.[16] During cement production, sources of calcium oxide and silica are finely ground, mixed, and pyro processed, or subjected to high temperatures. During this step, calcium oxide and silica react to form dicalcium silicate.[17] However, not all of the calcium oxide is consumed in the reaction and reacts with the intermediate dicalcium silicate to form Tricalcium silicate, leaving excess calcium oxide. Oftentimes, there is again excess calcium oxide remaining in the cement clinker, known as "free lime".[18] During hydration, water reacts with this free lime to form calcium hydroxide, a preliminary reaction of the hydration process:

$$CaO + H_2O \rightarrow Ca(OH)_2$$

In addition to the hydration of free lime C_3S and C_2S will also hydrate, producing the binding materials that give concrete its strength.

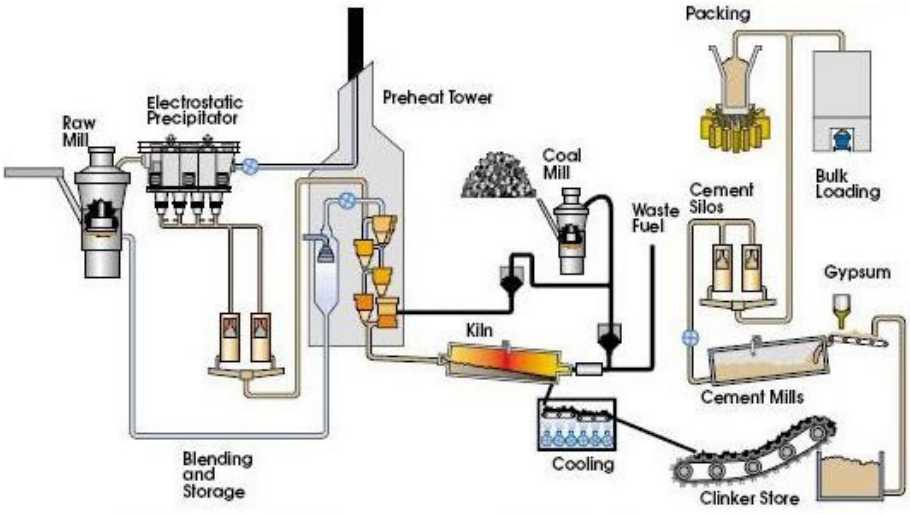

Figure 1. Cement production process.

When packaged, the Portland cement is anhydrous.[19] In order to produce concrete, the Portland cement is mixed with sand, gravel and water. When mixed with water, a hydration reaction occurs involving multiple reactions, where the products of the intermediates bond to form a solid mass.

Results and Discussion. Table 1 contains each sample with according ratio, and the pressure required to break the cement. These findings are graphed in Figure 3, which demonstrate the increase in strength with addition of lime. The dried cement samples, indented where the force probe was, are shown in Figure 4.

Sample #	Percent CaO	Percent Basalt	Percent Water	Pascals Required
1	5%	70%	25%	8.14MPa
2	5%	70%	25%	7.47MPa
3	10%	65%	25%	8.98MPa
4	15%	60%	25%	9.77MPa
5	20%	55%	25%	11.67 MPa
6	25%	50%	25%	>14.82MPa
7	60%	0%	40%	>14.82MPa

Table 1. Ratios tested and the according pascals required to break the cement.

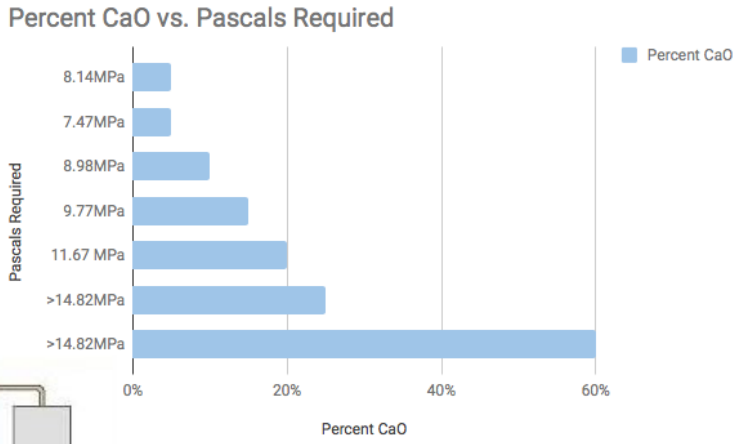

Figure 3. Relationship between the percentage of calcium oxide and the Pascals required to break the cement.

These results shown in both the table and graph demonstrate how the addition of lime strengthens the cement. However, after 25%, the samples require similar amounts of force to break, since basalt contributes an additional 10% CaO. If 25% of lime were used in the production of cement instead of the 60% found in Portland cement now, 3.9375 x 10^8 tons of carbon dioxide would be conserved, according to the following calculation:

$(2.25x10^2)(0.35) = 3.9375x10^8$ metric tons

Conclusion. In conclusion, replacing the majority of limestone in cement with basalt would be

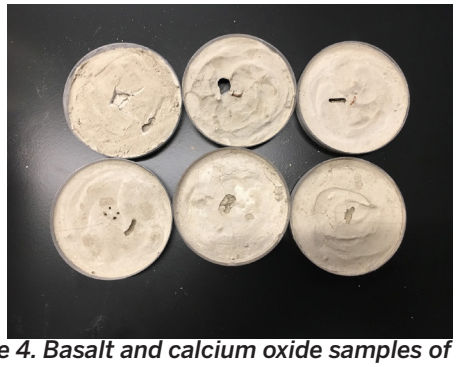

Figure 4. Basalt and calcium oxide samples of varying ratios. Percent calcium oxide for top row left to right: 25%, 20%, 15%. Bottom row left to right: 10%, 10%, 5%.

an ideal way to combat climate change. While the proposed solution would greatly reduce carbon emissions, there is an urgent need for further research in this field. Basalt is currently used predominantly as an aggregate for construction projects, as well as cut into thin slabs for tiles and other stone objects, but so far has had limited use as the primary component of cement.[21] Research should be conducted on the carbon sequestration properties of basalt, and how this could both positively and negatively affect the outcome. While climate change will continue to progress, the use of basalt in cement would make a contribution that might mitigate the effects of climate change in the long term.

Methods and Materials. In order to validate the usability of basalt as an alternative to limestone, multiple experiments were conducted to establish valid ratios of basalt to calcium oxide. The basalt and calcium oxide were ordered online, from Alibaba group and Carolina Biological Supplies Company respectively. The goal of this experiment was to produce a strong cement with as little calcium oxide possible. To do so, five different ratios were tested, starting with 5% calcium oxide and increasing the amount by intervals of 5% until a suitable result was acquired. The water content was held at a constant 25% of the mixture, and the basalt changed according to the percent calcium oxide. Each sample was measured using a 1:1 ratio of grams to mL, the total amount being 100 per sample.

For the first sample, 5 grams of calcium oxide was weighed and then added to a plastic container. This was followed by 25 mL of water, and 70g of basalt. The sample was then mixed with a metal stirrer and poured into half a petri dish. Immediately after pouring, the samples were set aside to dry for 24 hours. These steps were repeated for all the ratios, weighing all the components accordingly as laid out in the table below. The samples were all compared to Portland cement, which has 60% CaO. [18]

In order to test the strength of the cement, Vernier dual range force sensors were used to measure the amount of force required to break each sample. After the samples were dry, pressure was applied to each sample by the head of the sensor, recording the amount of force applied. Constant and increasing force was applied, and the force required to break the sample was recorded. This step was conducted for every single sample. In order to convert the force applied into Pascals to measure pressure, the measured newtons were divided by the area of the head of the sensor. This area was estimated to be about 4mm^2.

The final amount of estimated carbon dioxide saved was calculated by dividing the original 2.25 x 10^9 tons of carbon dioxide by 2, to find the amount of carbon dioxide released from the calcination process. Then, 35% of this value was found to be the amount of carbon dioxide saved. This value was calculated under the hypothesis that using only 25% calcium oxide would save 35% of the total carbon dioxide emissions due to calcination.

Acknowledgements. This research was supported with materials by Avenues: New York. I thank my teachers from Avenues: New York, who continuously encouraged me throughout my research despite initial obstacles. I would especially like to express my gratitude towards Pedro Jofre Lora, for fostering an environment which welcomed curiosity, and granted me the opportunity to start this research. Finally, I am immensely grateful to Denise Reitz, for being a dedicated supervisor, mentor, and inspiration throughout this entire process.

References.

1. Houghton, J. T. et al. (eds) Climate Change 1995: The Science of Climate Change(Cambridge Univ. Press, Cambridge, 1996).

2. Andrew, R. M.: Global CO2 emissions from cement production, Earth Syst. Sci. Data, 10, 195-217, https://doi.org/10.5194/essd-10-195-2018, 2018.

3. Felder-Casagrande, S.; Wiedemann, H. G.; Reller, A. *Journal of thermal analysis* **1997**, 49 (2), 971–978.

4. Rubenstein, M. Emissions from the Cement Industry http://blogs.ei.columbia.edu/2012/05/09/emissions-from-the-cement-industry/ (accessed May 1, 2017).

5. Olivier JGJ et al. (2015), Trends in global CO2 emissions; 2015 Report, The Hague: PBL Netherlands Environmental Assessment Agency; Ispra: European Commission, Joint Research Centre.

6. Ibid

7. Yan, W.; Feng, Y. L.; Yu, M. G.; Chao, Y. H. *Advanced Materials Research* **2012**, 518-523, 701–704.

8. Fly Ash (Tech. No. #C850321). (1985). Aberdeen Group

9. Almuammar, A.; Bernal, R.; Sonvane, R.; Geer, S.; Davis, P.; Sambhaji; Carleton, E.; Dheeraj; Fedorka, B.; Kudzin, A.; Yeshwanth; Uma; Umair; Haitham; Dale; Birdawade, Y.; Ay, A.; Rodriguez, J.; Babbar, R. K.; Mason Nichols; AJINKY; ASP. yogesh https://precast.org/2010/05/using-fly-ash-in-concrete/ (accessed May 12, 2017).

10. Britannica, T. E. of E. Basalt https://www.britannica.com/science/basalt (accessed May 1, 2017).

11. Thomas, J.; Jennings, H. 3.6 - Mineral and Oxide Composition of Portland Cement http://iti.northwestern.edu/cement/monograph/Monograph3_6.html (accessed May 11, 2017).

12. Zych, T.; Wojciech, K. Brittle Matrix Composites 10 **2012**, 155–166.

13. Liu, Fengjuan, "Early-age hydration studies of Portland cement" (2014). Electronic eses and

Dissertations. Paper 1753. h ps://doi.org/10.18297/etd/1753

14 Liu, F.; Lan, M. Z. Key Engineering Materials **2012**, 509, 20–25.

15. How Concrete is Made http://www.cement.org/cement-concrete-applications/how-concrete-is-made (accessed May 11, 2018).

16. 5.1 - Overview of the Concrete Hydration Process http://iti.northwestern.edu/cement/monograph/Monograph5_1.html (accessed Aug 21, 2018).

17. http://www.cement.org/cement-concrete-applications/how-cement-is-made

18. Brown, P. W. Early-Age Cement Hydration Reactions http://www.bing.com/cr?IG=646F807D0ADF4C138A6EC0730B60D079&CID=0F1C2706FE3A69721889 2B3EFFC76828&rd=1&h=HdTFnvfb2Bh_WT2fJ_SkN_NTdwvY1ShQpUaY7PZ56ok&v=1&r=http://onlinepubs.trb.org/Onlinepubs/trr/1990/1284/1284-007.pdf&p=DevEx.LB.1,5068.1(accessed May 26, 2017).

DOI: here
Reference here

19 Cement hydration https://www.understanding-cement.com/hydration.html (accessed Aug 21, 2018).

20 Nigeria Crusher http://www.fijihotelsnadi.com/solutions/mineral-plant/cement-manufacturing-process-flow-chart.html (accessed Aug 21, 2018).

21 Lea, F. M.; Mason, T. O. Cement https://www.britannica.com/technology/cement-building-material (accessed May 25, 2017).

22 King, H. M. Basalt https://geology.com/rocks/basalt.shtml (accessed Aug 21, 2018).

Author. Sophia Shapiro is an aspiring environmental engineer from New York City. She was awarded a bronze medal at Genius Olympiad, an international environmental science competition. In addition to sustainable cement, Sophia is also interested in sustainable lead filtration, computer programming, and entrepreneurship.

Investigation of schizophrenia factors in human neurons

Ryan M. Onatzevitch

Yorktown High School, 2727 Crompond Road, Yorktown Heights, NY, 10598, USA

ryan.onatzevitch@yorktown.org

ABSTRACT: Schizophrenia is a prevalent neuropsychiatric disorder with a high heritability rate. This heritability rate is attributed to genetic risk factors. The most influential risk factor that has been identified so far is the gene NRXN1. Defects in this gene are found in much higher rates in schizophrenia patients, identifying it as a risk factor. The neurexin protein is involved in neurotransmission, cellular recognition, and neuron development. To investigate the effects of schizophrenia in neurons, cells were used from established schizophrenic lines. These cells were cultured into developed neurons and studied for neuronal migration, astrocyte ratios, and NRXN1 isoform expression. Gene expression was studied through RNA sequencing, and cells were imaged with confocal laser microscopy. Neuronal migration changed significantly along with ratios of astrocytes to neurons, and isoform expression was shown to be altered in schizophrenic lines as well. Observations of these specific functional changes offer more insight into the mechanics of schizophrenia as well as the reliability of cell-based disease studies.

KEYWORDS: Biology; Schizophrenia; Stem Cells; Neurons; Neuronal Migration

Introduction. Schizophrenia is a debilitating and chronic mental disorder that results in a wide variety of symptoms including hallucinations, delusions, and paranoia. It affects large numbers of people with a global prevalence rate of 1% and a rate of 1.2% in the US with 3.2 million Americans having the disorder.[1] In addition to this, current treatment options for schizophrenia are insufficient with very unfavorable side effects.[2] These issues stem from the overall lack of understanding concerning the causes of the disorder. Genes related to schizophrenia such as *NRXN1* have been shown to influence neuronal migration as well as the other types of cells in the brain, but it is unknown how those changes relate to the disorder.[3] In addition to *NRXN1*, many of the other potential genes associated with increased risk for schizophrenia require further functional studies to determine their specific relation to the disorder. The goals of this research were to investigate the changes in neuronal migration and cell type composition that occur in patients with schizophrenia harboring heterozygous deletions in *NRXN1*, as well as investigate changes in the mRNA expression of *NRXN1*. This work may help determine what cellular phenotypes change and may provide more insight towards the actual causes of the disease.

Review of Literature. Past schizophrenia research has identified a set of specific changes that may be related to the development of the disorder. Previously established changes occur within the processes of neuronal migration4 and the ratios of neurons to supporting cells.[5] Both processes are altered in schizophrenic patients and may relate to the disorder.

Neuronal Migration and Glial Cells. Neuronal migration is a vital part of the development of the brain that contributes to growth and later function. Supporting cells such as astrocytes and oligodendrocytes greatly contribute to this process. As the brain develops, neurons can migrate radially or tangentially to form the various structures in the brain. This process is vital for the proper functioning of the brain as it is the driving force behind early development and establishment of proper neuronal circuits.[4,6] Previous animal studies have shown that neuronal migration is defective in models of schizophrenia, but the mechanism has not been identified yet. The relationship between neuronal and supporting glial cells is further implicated as the genes related to these cells have altered expression in patients with schizophrenia compared to controls, which could contribute to differences in the ratios of each cell type in the brain.[6]

NRXN1 Gene. Deletions in *NRXN1* have been shown to be associated with schizophrenia through a greatly increased rate of deletions in patient populations.[7,8] Previous studies investigated copy number variations (CNV) which are duplications or deletions over 100kb in the genome. Patients carrying CNVs in this gene have been shown to have a much higher risk for developing neurological disorders such as schizophrenia. This gene has a number of alternate splicing sites which allows the

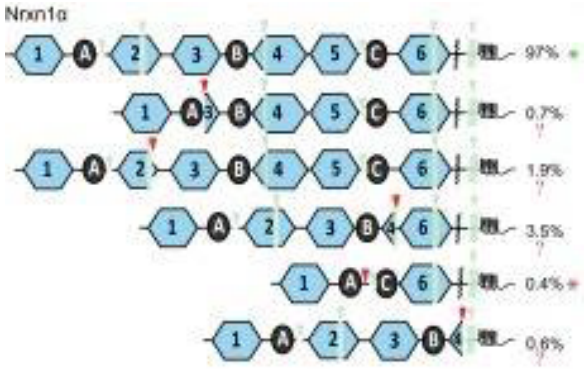

Figure 1. A chart showing isoforms of the gene and their relative prevalences[7].

DOI: here
Reference here

gene to be expressed in different sequences called isoforms,[9] and mouse studies have shown a very large number of *NRXN1* isoforms that are expressed normally. Figure 1 shows some of the possible configurations for the exons in *NRXN1*.

Some of these isoforms have already been identified in mice but many possible isoforms have not been identified in humans. In addition to this, past research has failed to compare the isoforms found in schizophrenia patients to those found in controls. Investigating a link between changes in isoform expression with neuronal migration and cell type composition may provide more information relating to the development of schizophrenia and new pathways to target for treatment.

Current issues with schizophrenia research are mostly due to the lack of information relating specific mechanical changes and the psychological symptoms that occur in the disease. This result in difficulty creating new and effective treatment options for schizophrenia. This project investigated three phenotypic changes that occurred in patients exhibiting psychosis who harbor deletions in the gene *NRXN1*, using a variety of established cell lines side-by-side in comparisons. By looking at the functional changes that occur in these patient cell lines it may be possible to form a more complete view of the disease, possibly leading to new and effective methods of treatment and diagnosis.

The issues addressed in this study are:

- The relationship between neuronal migration and patients with *NRXN1* deletions has not been established.
- Imbalances in the ratios between neural and supporting cells are related to schizophrenia but the cause behind this relationship has not been identified.
- The gene *NRXN1* has multiple isoforms and the expression of these isoforms has not been studied in relation to schizophrenia.

The goals of this study are:

- Investigate changes in neuronal migration that occur within patient versus control lines.
- Quantify the ratios of neural and supporting cells that are found in control and patient cell lines.
- Identify various isoforms of *NRXN1* found in patient versus control cell cultures.

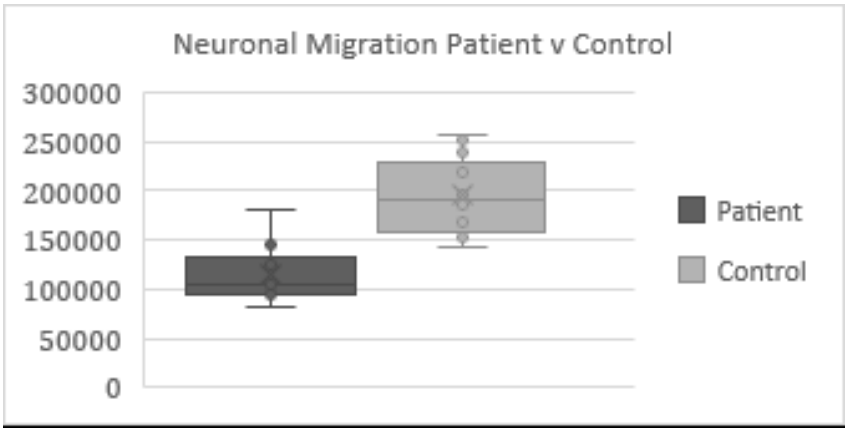

Figure 5. Box-and-whisker chart showing reuronal migration data in square pixels.

Results.

Neurosphere Assay. The measured neurospheres were processed using ImageJ and the resulting figures were analyzed using Excel and organized into data tables. The data set included three patient lines (972, 973, 641) and two control lines (2607, 553) with twelve analyzed neurospheres from each line. Average neuronal migration increased from 114,700 square pixels in patient lines to 196,300 square pixels in control lines ($p < .001$) (Figure 5). This significant 71% increase indicates that neuronal migration is decreased in patient line neurospheres. P values also reached significance when comparing cell lines directly instead of grouped as patients and controls showing a stronger relationship between lines. There were a small number of discarded results due to abnormal growth, multiple neurosphere placement, and placement close to the plate wall. In addition, variance in neurosphere size may have been another source of error. The method of statistical analysis used was a 2-sample t-test.

Astrocyte Quantification. This experiment measured the percentage area covered by a thresholded stain of an astrocyte marker, a neuron marker, and a marker for all genetic material used for normalization. Measurements were normalized to the DAPI blue stain and subjected to a two-sample t- test. There was a significant difference in the astrocyte-neuron results for patient versus control lines. ($p=.048$). Normalization to DAPI blue ensures that the ratio is not influenced by the number of cells in the image, and each of the 32 slides were imaged in two separate areas to ensure accuracy. However, the actual difference in means was not extremely large with an average difference of -.39 ± .20 (Figure 6).

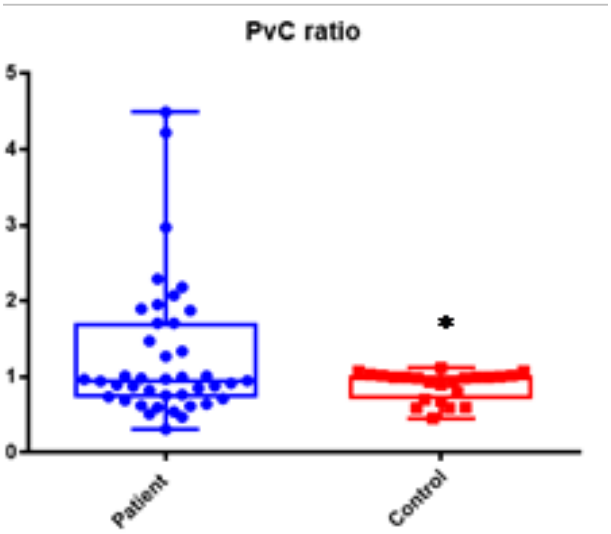

Figure 6. Ratio data points in patients and control groups.

Isoform Identification. In this section of the experiment we sequenced RNA from a number of cell lines and compared the data to a database sample taken from NCBI of *Homo sapiens NRXN1* alpha (Accession number: NM_004801.) Snapgene was then used to align the sequences and identify exons missing from the sequenced

samples. The sequencing process used multiple primers due to the length of RNA samples. Identified isoforms differed from the comparison sequence in numerous ways including deletions of exon 2 and various other insertions. There were four separate isoforms that were identified with certain isoforms only appearing in the RNA samples taken from the patient cell cultures and not present in the control cultures, showing a change in genetic structure between the schizophrenia patients and healthy controls. Although the sample size is relatively small, these findings still contribute to the observed changes in the structure of this gene in humans with schizophrenia.

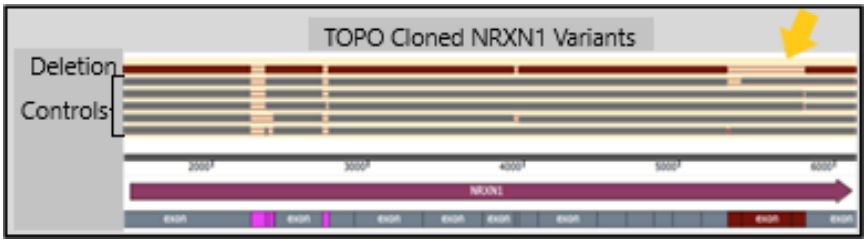

Figure 7. Sequencing data with highlighted deletion of exon 7, figure provided by mentor.

Conclusion. The two-sample t-test related to the neuronal migration experiment demonstrated a highly significant change in the distance migrated radially by each neurosphere. Such a significant increase in neurosphere migration is indicative of a change in the functioning of neuronal migration, a key aspect of neural development that is vital for proper functioning of the brain. These results mirror what has been observed in past animal and postmortem studies using models of schizophrenia as well as schizophrenic cells.[4] The consistent results confirm these findings as a mechanical symptom of schizophrenia as well as reinforcing the consistency of using stem cell cultures in order to study aspects of schizophrenia. Defects in this process have already been associated with other neuropsychiatric disorders in the past, and this experiment reinforces the relationship between schizophrenia and neuronal migration. The results support the original hypothesis that neuronal migration would be much more pronounced and functional in the control lines when compared to the patient lines.

The results for astrocyte quantification showed a significant increase in the ratios found in patient lines when compared to controls. The results indicate that the sampled cell cultures decreased in ratio of astrocytes to neurons in controls which refutes previous studies.[6] However, there were numerous sources of error such as issues in culture setup, staining method, and imaging technique that could contribute to these results. In addition to this, the results barely reached significance but there is not enough information to definitively refute or support the original hypothesis that the ratio would decrease in patient cell lines compared to controls. There is also variance between types of schizophrenia concerning change in astrocyte ratios which could have contributed to the inconsistent results.

The isoform identification portion of this experiment succeeded in isolating and sequencing a number of alternative isoforms from a wide number of cell cultures from patient and control lines. There were consistent patterns found in the deletion and insertion of exons and intron sequences of the genes which shows a change in the resulting variable expression that occurs due to the multiple splice sites. By identifying these isoforms this experiment validates the findings that variable expression is affected by the presence of schizophrenia in patient lines and reinforces the findings of past studies concerning isoform expression.[9,11] However, the sample size in this experiment was somewhat reduced due to primer and sequencing errors. The original hypothesis was partially supported by the identification of alternative isoforms, but additional validation is required to accurately categorize the isoforms.

Methodology. This experiment primarily involved three experimental assays used to quantify data related to isoforms, neuronal migration, and astrocyte ratios in cell cultures to investigate changes in patients harboring *NRXN1* deletions. For the identification of isoforms, RNA was extracted using a liquid-liquid technique involving phenol and chloroform. The extracted RNA was sequenced using long-read sequencing and compared to an original *NRXN1* sequence in order to identify different isoforms. The neuronal migration assay was performed by allowing progenitor cells to form neurospheres in culture. These spheres were allowed to migrate across a plate and the resulting spread of cells was quantified and measured across cell lines. The astrocyte ratios were measured by staining cell cultures with markers for astrocytes, neurons, and all cells. The cells were imaged in three colors in order to quantify the ratios of each type of cell in the culture in order to compare the areas taken up on the image by each stain separately.

Neurosphere assay. Neurospheres are clumps of a few hundred cells that form naturally when neurons are grown in free-floating culture. The starting cells are taken from a stock of pre-modified pluripotent cells and plated. They begin to differentiate naturally and consist of a heterogeneous mix of cell types and stages of development. These neurospheres are utilized to measure the natural movement of neurons as they grow. In order to generate useable neurospheres, the mentor plated groups of neural progenitor cells in non-adherent plates and allowed them to aggregate for 48 hours. The student prepared a 96-well

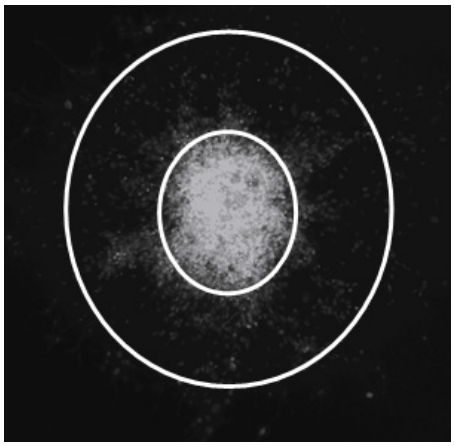

Figure 3. Example neurosphere assay with circles showing approximate inner and outer measurements.

DOI: here
Reference here

plate with a Matrigel coating and picked similar sized neurospheres into the plate using a pipette. Each neurosphere was centered in the plate by the student and checked for a single neurosphere in each well. Migration occurred for 48 hours and the cells were fixed with a 4% paraformaldehyde solution and stained using DAPI, a nuclear DNA stain, to allow for imaging.[10] Cells were imaged using an epifluorescence microscope and the resulting images were quantified using ImageJ, an image processing software. This allows for quantification of the original size of the neurosphere compared to the size after the 48-hour migration period.[10] Figure 2 shows the approximate points of measurement used for the inner and outer boundaries. This method allows for the comparison of distance covered by the cells migrating, obtained by subtracting the original distance from the migrated distance. This method effectively quantifies and indicates the presence of neuronal migration. [10]

Isoform identification. For the identification of RNA isoforms, the mentor prepared a culture of hiPSC neurons in 6-well plates and stored them in an incubator. The cell cultures were lysed using 1mL TRIzol per well, a solution containing phenol. The TRIzol and cells were mixed with 150 µL chloroform and centrifuged in order to separate the cellular components from RNA. Figure 3 shows the phase separation after centrifuging. The aqueous phase that contains RNA in solution was transferred to another container with isopropanol and centrifuged to pellet the RNA. The resulting pellet was washed using ethanol and resuspended in water for storage. This method was taken from the TRIzol Reagent User Guide from Thermo Fischer Scientific. The purified RNA was used to create a complimentary cDNA. This cDNA was used in a PCR with a forward and reverse primer targeting the first and last exons of *NRXN1*, respectively. The PCR products were separated through gel electrophoresis, extracted, and purified. The resulting sample was ligated with a TOPO vector that resulted in a complete plasmid ring that could be transformed into bacteria for culturing. The bacteria were then harvested, and RNA purified with a Thermo-Fischer miniprep. This purified RNA was sent to GENEWIZ for Sanger sequencing using their proprietary method. A gene sequence software called GENEWIZ was then used to compare the resulting sequences and identify differing isoforms by aligning them to a comparison sequence and identifying missing exons or inserted exons which indicates a differing isoform.[9]

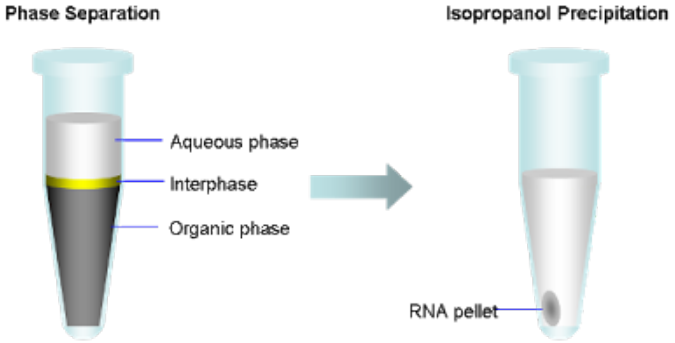

Figure 3. Showing phase separation of reagents, the aqueous phase contains RNA from molecularhub.blogspot.com

Astrocyte quantification. The method for quantification of astrocyte ratios utilizes three markers that stain for astrocytes, neurons, and all nuclei. A primary antibody was used to target s100b and MAP2 followed by a secondary antibody with an attached fluorescent probe for either GFP or RFP, two fluorescent proteins. The dyes used were GFP, RFP and DAPI blue which all fluoresce under differing wavelengths targeting s100b (glial-specific protein), MAP-2 (neural specific protein) and DAPI (all genetic material) respectively (Figure 4). The prepared cultures were grown from different neural progenitor lines by the mentor and placed on microscope slides for imaging. Each slide was imaged on a Zeiss LSM 780 confocal microscope using an automated z-stack program that allows for the imaging of multiple layers of cells simultaneously. Each section of cells was imaged under three wavelengths (395 nm, 588nm, and 358nm for GFP, RFP, and DAPI respectively) in order to measure each dye separately. Methods for this section were provided by the mentor and developed independently in the lab. This allowed for three separate images of the same section of cells each highlighting either all neurons, all astrocytes, and all genetic material in both types of cells. The resulting images were quantified using ImageJ and normalized to the DAPI dye in order to obtain a ratio of neurons to astrocytes which was compared across cell lines. Each image was separated into channels and thresholded to produce a black-and-white image to quantify the surface area occupied by each channel. The surface areas were then normalized to the DAPI blue and analyzed in Prism Graphpad.

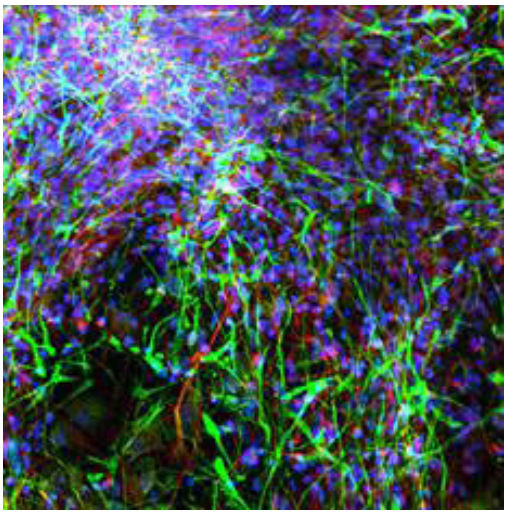

Figure 4. A composite image showing the three channels before separation and thresholding.

Acknowledgements. I would like to thank Dr. Kristen Brennand and Dr. Erin Flaherty for their guidance and support during my research, as well as Mr. Michael Blueglass and Ms. Rachel Koenigstein for overseeing my school science research program. I would also like to thank my family for their continued support.

References.

1. National Institute Mental Health. https://www.nimh.nih.gov/health/topics/schizophrenia/index.shtml (accessed July 10, 2017).

2. Patel, KR; Cherian, J; Gohil, K; Atkinson, D. Schizophrenia: Overview and Treatment Options. P&T. **2014**, 39(9), 638-645.

3. Craig, AM; Kang, Y. Neurexin-Neuroligin Signaling in Synapse Development. *Curr. Opin. Neurobiol.* **2007**, 17(1), 43-52.

4. Muraki, K; Tanigaki, K. Neuronal Migration Abnormalities and Its Possible Implications for Schizophrenia. *Front. Neurosci.* **2015**, 9(74), 1-10.

5. Sherwood, CC; Stimpson, CD; Raghanti, MA; Wildman, DE; Uddin, M; Grossman, LI; Goodman, M; Redmond, JC; Bonar, CJ; Erwin, JM; Hof, PR. Evolution of Increased Glia-Neuron Ratios in the Human Frontal Cortex. *Proc. Natl. Acad. Sci.* **2006**,103(37),13606–13611.

6. Wang, C; Aleksic, B; Ozaki, N. Glia-related Genes and their contribution to Schizophrenia. P*sychiatry Clin Neurosci.* **2015**, 69 (8), 448–461.

7. Kirov, G; Rujescu, D; Ingason, A; Collier, DA; O'Donovan, MC; Owen, MJ. Neurexin 1 (NRXN1) Deletions in Schizophrenia. *Schizophr. Bull.* **2009**, 35 (5), 851-854.

8. Kirov, G. CNVs in Neuropsychiatric Disorders. *Hum. Mol. Genet.* **2015**, 24 (R1), R45-49.

9. Treutlein, B; Gokze, O; Quake, SR; Sudhof, TC. Cartography of Neurexin Alternative Splicing Mapped by Single-Molecule Long-Read MRNA Sequencing. *Proc. Natl. Acad. Sci.* **2014**, 111(13) E1291-1299.

10. Topol, A; Tran, NN; Brennand, KJ. A Guide to Generating and Using hiPSC Derived NPCs for the Study of Neurological Diseases. *J. Vis. Exp*. [Online] **2015**, 96, e52495, https://www.ncbi.nlm.nih.gov/pmc/articles/PMC4354663/ (accessed July 24, 2017).

11. Chih, B; Gollan, L; Scheiffele, P. Alternative Splicing Controls Selective Trans-Synaptic Interactions of the Neuroligin-Neurexin Complex. *Neuron.* **2006**, 51(2),171–178.

Author. Ryan Onatzevitch is a senior at Yorktown High School who has participated in science research for three years. He is a three-season track and field athlete, as well as an avid participant in the high school band program on trumpet. Ryan will be studying biology at Johns Hopkins University.

DOI: here
Reference here

Study of Cutting the Möbius

Ekaterina Y. Arutyunova

Pope High School, 3001 Hembree Road, Marietta, GA, 30062, USA

ekaterina.arutyunova2001@gmail.com

ABSTRACT: The paradox of cutting the Möbius strip is that longitudinal cutting is ambiguous, unlike a cylindrical surface. The configurations and geometrical dimensions of the obtained strips depend on the distance from the cut to the edge of the surface. For example, if there was cutting into one-sixth of the width of a cylindrical surface, it will result in two separate cylindrical surfaces of different widths. This is different with a Möbius strip: if there was cutting into one-sixth of the width of a Möbius surface, it produces two connected strips. One of the strips is twice as large as the original Möbius strip and has 3 twists, and the second one is the same as initial Möbius strip. To date, the parameters and characteristics of the Möbius strip have been reliably identified, which determine the ambiguity of the cutting result, unlike a cylindrical surface.

The interest in the cutting paradox is of both scientific and of practical interest for cardiac surgery. If we manage to resolve this paradox, that is, to find out what parameters and characteristics lead to the ambiguity of the cutting, this will solve one of the problems in cardiac surgery.

Thus, the problem (of which the solution is described in this article) is the identification, experimentally and theoretically, of factors that determine the uniqueness of the configurations obtained by cutting a Möbius strip and studying the resulting configurations

KEYWORDS: Topology; Cylindrical surface; Möbius Strip; One-sided Surface; Surface cutting

Introduction. The study of geometric properties and spatial relations unaffected by the continuous change of shape or size of figures is called Topology. In this article we will discuss the study of geometric properties of a Möbius strip. The Möbius strip, also called the Möbius loop is a model that can be obtained by turning a long strip of paper a half turn and then connecting its ends together.[1]

The father of the Möbius strip is August Ferdinand Möbius, a student of Gauss. He wrote numerous works on geometry but became famous for the discovery of a one-sided surface in 1858.

Cylindrical Surface and Möbius Strip. For a better understanding of the differences in the Möbius strip from the usual cylindrical surface, it is necessary to directly compare them.

If one puts a finger on the side of the cylindrical surface and moves it endlessly without lifting one's finger from the surface, the movement will take place only on one side. To get to the other side of a cylindrical surface, there is need to remove one's finger and put it on the second side. This is different with a Möbius strip; if one puts a finger on the side of the cylindrical surface and moves it endlessly without lifting one's finger from the surface, the movement will take place on both sides of surface. It means that the cylindrical surface is double-sided and has a discontinuous surface while the Möbius strip is one-sided and with a continuous surface.

Also, the surface is orientable if it has two sides. As already known, the cylindrical surface has two sides, so it is orientable and the Möbius surface is not orientable.

From the comparison it can be seen that the cylindrical surface and the Möbius surface are completely different geometric objects, although they are made of a similar long strip.

Cutting a Cylindrical Surface and Möbius Strip. As is already known, any longitudinal cutting of a cylindrical surface gives two cylinders of different heights. Subsequent to the longitudinal cutting of a Möbius strip, the resulting shapes have completely different configurations depending on the distance from the scissors to the edge of the strip.[2] This paradox is especially interesting for many topologists.[3]

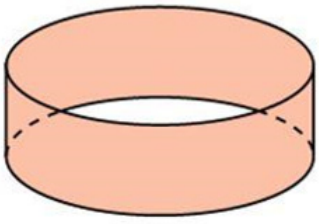

Figure 1. The image of a cylindrical surface.

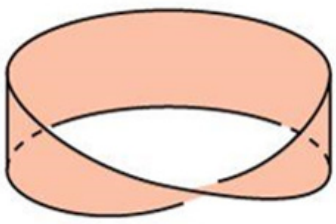

Figure 2. The image of the Möbius strip.

DOI: here
Reference here

Characteristics of the cylindrical surface	Characteristics of the Möbius strip
Double-sided surface	One-sided surface
Noncontinuity	Continuity
Orientable	Not orientable

Table 1. Geometrical and topologial characteristics of the cylindrical surface and Möbius strip.

This experiment was repeated to compare the obtained shapes in the longitudinal cutting of a cylindrical surface and a Möbius strip. The researcher hypothesizes that after experiments and studying the obtained geometric figures, the paradox can be explained analytically using the condition of the proportionality between the area (S) of the Möbius strip and width of the Möbius strip (λ), the radius of the circle forming the Möbius strip (R), the condition of the proportionality between the length of the edge (L) and the width of the Möbius strip (λ), as well as radius of the circle forming the Möbius strip (R).

Methods. To begin with, initial samples of a cylindrical surface and a Möbius strip were made from strips of paper of equal length and width (Figure 3).[4] For ease of cutting and making models, striped paper was used.

Figure 3. Original surfaces: Cylindrical surface and Möbius strip.

Experiment #1. After preparing the models, the longitudinal cutting of the two surfaces begins by cutting into one-sixth of the initial width. As can be seen from the experiment, two cylindrical surfaces of different widths were obtained by longitudinal cutting of the cylindrical surface. By splitting the Möbius surface longitudinally, two connected strips were obtained: one twice as large as the original Möbius strip and with 3 twists, and one initial Möbius strip (Figure 4).

Figure 4. Experimental results in longitudinal cutting of the cylindrical surface and Möbius surface by one-sixth of the initial strip width.

Experiment #2. Next, we increase the cut strip to one-fifth of the initial width of the strip. From the experiment, two cylindrical surfaces of different widths were obtained by the longitudinal cutting of the cylindrical surface. At longitudinal cutting of the Möbius surface, two connected tapes were obtained: one twice as large as the original Möbius strip and with 2 twists, and one Möbius strip of the original size (Figure 5).

Figure 5. Experimental results in longitudinal cutting of the cylindrical surface and Möbius surface by one-fifth of the initial width of the strip.

Experiment #3. Next, we cut the cylindrical surface and the Möbius surface longitudinally, retreating from the edge of the strip by one-fourth of the original strip width. From the experimental results it can be seen that cutting a cylindrical surface, two new cylindrical surfaces of different heights were obtained. When cutting the Möbius surface, two connected strips were obtained again: one twice as large as the original Möbius strip and with 2 twists, and one Möbius strip of the original size.

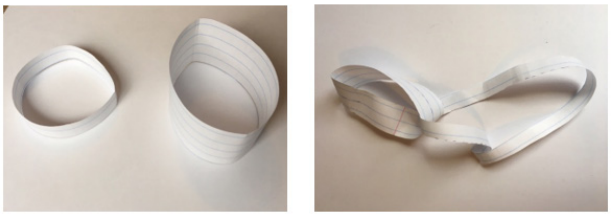

Figure 6. Experimental results in longitudinal cutting of the cylindrical surface and Möbius surface by one-fourth of the initial strip width.

Experiment #4. Next, we cut the cylindrical surface and the Möbius surface longitudinally, retreating from the edge of the strip by one-third of the initial strip width. From the experimental results it can be seen that cutting the cylindrical surface, two new cylindrical surfaces of different heights were obtained. When cutting the Möbius surface, two connected strips were obtained: one twice as large as the original Möbius strip and with 3 twists, and one Möbius strip of the original size.

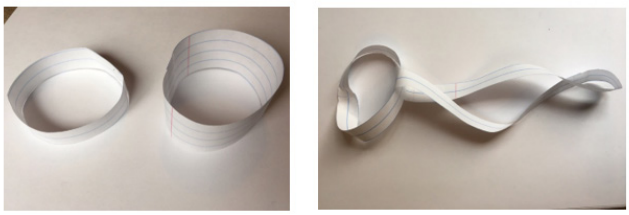

Figure 7. Experimental results in longitudinal cutting of the cylindrical surface and Möbius surface by one-third of the original strip width.

Experiment #5. In the last experiment, we cut the cylindrical surface and the Möbius surface in half, lengthwise. From

DOI: here
Reference here

the results of the experiment it is seen that by cutting a cylindrical surface in half, two equal cylinders were obtained. When cutting the Möbius surface in half, one surface was obtained. This surface is twice in length of the original Möbius surface and has 4 twists.

Figure 8. Experimental results in longitudinal cutting of the cylindrical surface and Möbius surface in half.

Results and Discussion. Following the results of five experiments with cutting a cylindrical surface and Möbius surface, the summarizing result is shown in Table 2.

Experiment Results # 1-5

№	Experiment Description	The result of cutting the cylindrical surface	The result of cutting the Möbius surface
1	Cut into one-sixth	Two cylindrical surfaces of different heights	Two connected strips: one twice as large as the Möbius strip and with 3 twists, and one Möbius strip of the original size
2	Cut into one-fifth	Two cylindrical surfaces of different heights	Two connected strips: one twice as large as the Möbius strip and with 2 twists, and one Möbius strip of the original size
3	Cut into one-fourth	Two cylindrical surfaces of different heights	Two connected strips: one twice as large as the Möbius strip and with 2 twists, and one Möbius strip of the original size
4	Cut into one-third	Two cylindrical surfaces of different heights	Two connected strips: one twice as large as the Möbius strip and with 3 twists, and one Möbius strip of the original size
5	Cut in half	Two cylindrical surfaces of equal height	One strip, twice the original with 4 twists

Table 2. Table of the experimental results of cutting the cylindrical surface and the Möbius surface in different ways.

From the table, it is possible to predict what will happen with the longitudinal cutting of a cylindrical surface. It is impossible to guess what happens with different longitudinal cutting of the Möbius strip.

Explanation of the Paradox of Cutting a Möbius Strip. Analyzing the obtained experimental results, there is the question of the nature of this geometric topology paradox in experiments with the longitudinal cutting of the Möbius strip. One of the explanations for this paradox is to apply a condition of the proportionality between the area (S) of the Möbius strip and the width of the Möbius strip (λ), the radius of the circle forming the Möbius strip (R), and the condition of the proportionality between the length of the edge of the Möbius strip (L) and width of the Möbius strip (λ), and the radius of the circle forming the Möbius strip (R). These dependencies are obtained analytically (for the case λ << R).

Calculating the integral of *d*L, find the length of the edge:

$$L = L(\lambda) = 2R \int_{-1}^{1} \sqrt{\mu^2 + 4(1+\mu x)^2}\, \frac{dx}{\sqrt{1-x^2}} \qquad (1)$$

where $\mu = \frac{\lambda}{R}$. In particular, consider $\mu \ll 1$. Therefore,

$$L \approx 4\pi R\left(1 + \frac{\lambda^2}{8R^2}\right) \qquad (2)$$

The area of the Möbius strip is determined by the formula:

$$S = \int_{-\lambda}^{\lambda} d\lambda \int_{0}^{2\pi} \sqrt{\frac{\lambda^2}{4} + (R + \lambda \sin\frac{\varphi}{2})^2}\, d\varphi \qquad (3)$$

where (λ, φ) - orthogonal coordinates.

Comparing (1) and (3), can see that $S = \int_0^{\lambda} L(\lambda) d\lambda$, where L(λ) is determined in equation (1). In particular, in the limit of $\lambda \ll R$ (based on equation (2)) find:

$$S \approx 4\pi R\lambda\left(1 + \frac{\lambda^2}{24R^2}\right) \qquad (4)$$

If expression for area of Möbius strip presented as a sum of two terms:

$$S \approx 4\pi R\lambda + \frac{\pi\lambda^3}{6R}$$

, first linear term means area of original tape, which length is 2πR and width is 2λ and cubic term means the curvature of the surface.

Expressions (2) and (4) allow for the comparison of the geometric characteristics of the cylindrical surface and the Möbius surface having same cross section – circle of radius R.

Writing the conditions for preserving the length of the edge of the strip and the area of the strip for cylindrical surface and Möbius surface, one obtains a system of equations of the third degree with the number of unknowns equal to the number of bands which are obtained after cutting.

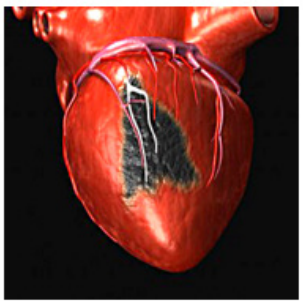

Figure 9. A cardiac muscle patch is used to treat myocardial infarction. It helps to restore damaged heart tissue.

The Impact of Cardiac Surgery. In cardiac surgery, there is a problem of determining the size, shape, and thickness of the material for the cardiac muscle patch, which is attached to the myocardium in the place of a scar from a myocardial infarction (Figure 9).

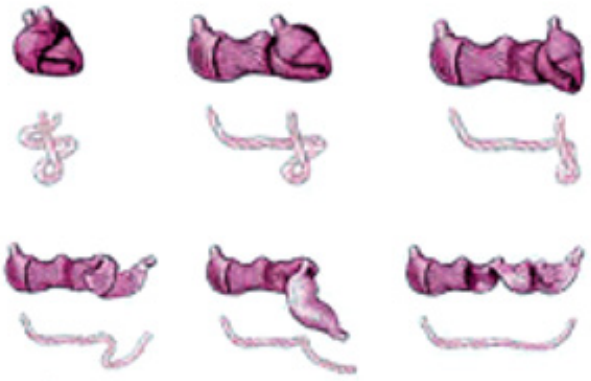

Figure 10. Myocardium is a curved-twisted strip with the topology of a Möbius Strip.

In accordance with the discovery of Dr. Francisco Torrent-Guasp and Dr. Gerald Buckberg myocardium is a thick curved-twisted strip with a Möbius strip topology (Figure 10).[5-6]

This cardiological discovery complicates the issue of determining the configuration of the patch (on the curved-twisted surface with the topology of a Möbius strip). During design and creating the cardiac muscle patch of a patient, the surgeon should consider ambiguity of the incision on the heart muscle. Ignoring this increases the risk of a patient's postoperative pathologies like aneurysm. The factor influencing the solution of this question is the paradox of cutting a Möbius strip.

Therefore, the results of the research described in this article can be applied in cardiac surgery to determine the configuration and size of the cardiac muscle patch.

Conclusion. This article describes the experimental and theoretical studies of the paradox of cutting a Möbius strip; comparison with the cutting of the cylindrical surface, and the generalization of the results. The consequence of this is the identified characteristics and parameters of the Möbius strip, the values of which determine the configuration and the geometric dimensions of the resulting figures after longitudinal cutting. Significant findings from experiments and analysis include the width of the cut strip during the longitudinal cutting of the Möbius strip.

The results of these studies have practical cardiac surgery significance.

Acknowledgements. I acknowledge my father, Yurii Arutyunov, for his help and support in research.

References.

1. Fuchs D. Möbius strip. Variations on the Old Theme. *J. Quantum*. 1979, *1*, 2-9.

2. Marushina T.D. Cutting tapes. Studies in the field of natural sciences. [Online] 2014, 7. http://science.snauka.ru/2014/07/7567 (accessed Feb 8, 2019).

3. Sangalov M.E. Using the experiment in the study of topological properties of surfaces, International scientific-practical. conference "Modern directions of theoretical and applied research '2011», Odessa, Black Sea, UA, 2011. "Modern directions of theoretical and applied research: Odessa, Black Sea, 2011; pp 73–77.

4. Kordemsky B. Topological experiments with their own hands. *J. Quantum*. 1974, 3, 73-75.

5. Buckberg G. Basic science review: the helix and the heart. *J Thorac Cardiovasc Surg.* 2002, 124(5), 863-83.

6. Kocica M.; Corno A.; Carreras-Costa F.; Ballester-Rodes M.; Moghbel M.; Cueva C.; Lackovic V.; Kanjuh V.; Torrent-Guasp F. The helical ventricular myocardial band: global, three-dimensional, functional architecture of the ventricular myocardium. *Eur. J. Cardio-thoracic surgery*. 2006, 4, 21-40.

Author. Ekaterina Arutyunova conducts research in the field of Physics and Mathematics with her father. She plans to continue and develop her science projects in college in the respective major.

DOI: here
Reference here

Enhancement of Dietary Content of Iron in Brassica oleracia Through Soil Alterations

Cynthia Chen

Greenwich High School, 10 Hillside Rd. Greenwhich, CT, USA

cynthiachen2010@gmail.com

ABSTRACT: It is difficult for vegetarians and vegans to obtain their necessary iron levels, as the ferric iron found only in plants is in a much less bio-available form compared to its ferrous counterpart in meat. In this research, Kale (*Brassica oleracia*) plants were used to increase iron absorption by altering soil chemical conditions. Samples of kale leaves were studied using Extended X-ray Absorption Fine Structure (EXAFS) and X-ray absorption Near Edge Structure (XANES) spectroscopies. We found that, while the chemical nature of the iron species does not change within different regions of the plant, the amount of iron varies significantly within the plant during different growth stages due to the absorption of different amounts of iron from the soil. With the presence of Arsenic in the soil, the iron absorption of the plants is reduced significantly. Therefore, the results suggest that arsenic-containing pesticides should not be applied during the growth of these plants. It was also observed that lowering the pH (< 7) of soil helps the absorption of iron into the plants. It is also noteworthy to point out that both ferric and ferrous iron are present in our plant samples.

KEYWORDS: Anemia; X-Ray absorption; Brassica oleracia; Arsenic; Soil pH; Iron absorption

Introduction. There are many different kinds of minerals found in the human body. Among them, iron is one of the most recognizable. Even though the amount of iron in an adult human is a little less than a teaspoon, iron deficiency can easily cause harmful effects on the body. Iron is an essential component of hemoglobin, an erythrocyte protein that transfers oxygen from the lungs to the tissues.[1] As a component of myoglobin, a protein that provides oxygen to the muscles, iron also supports metabolism.[2] In addition, iron is necessary for growth, development, normal cellular function, synthesis of some hormones and connective tissues[2,3] as well as an essential mineral for nervous system development and function.

Iron is a mineral that is naturally present in many foods, added to several food products, and available as a dietary supplement. Dietary iron has two main forms: Ferric (Fe^{3+}) and Ferrous (Fe^{2+}).[1] Plants and iron-fortified foods contain solely ferric iron, whereas meat, seafood, and poultry contain both types of iron.[2] Ferrous iron, in the form of reduced iron, is more bioavailable, and therefore easily absorbed. On the other hand, ferric iron is not easily absorbed by the body. It must be reduced to ferrous iron in order to be taken in by the duodenal entrocytes.[1]

Vegetarianism is the practice of abstaining from the consumption of meat (red meat, poultry, seafood, and the flesh of any other animal), and may also include abstention from by-products of animal slaughter.[3] Vegetarian diets typically contain similar levels of iron to non-vegetarian diets, but the iron has lower bioavailability than iron from meat sources,[1] and its absorption can sometimes be inhibited by other dietary constituents. Veganism, on the other hand, is both the practice of abstaining from the use of animal products, particularly in diet, and an associated philosophy that rejects the commodity status of animals.[4] The related vegan diets can often be higher in iron than vegetarian diets as dairy products are often low in iron. The amount of iron in vegetarians tends to be lower than that in non-vegetarians,[2] and various small studies report very high rates of iron deficiency among those groups.[5,6]

Currently, there are increasing numbers of people who choose to be either vegetarians or vegans due to a variety of reasons including: health issues, dwindling animal populations, and animal cruelty, among others. It has been shown that ferric iron contributes about 10% to 15% of total iron intakes in western populations.[7-9] Therefore, it would be very useful and practical to investigate various methods to increase the amount of iron in plants to reduce iron deficiency, especially for both vegetarians and vegans.

The purpose of this research is to provide a solution for combating the worldwide issue of anemia, a condition present in 2 *billion* people. Iron is an essential nutrient not only for humans, but also for all types of plants, which use iron for chlorophyll formation, RNA metabolism, and transpiration process regulation.[1,10] The presence of iron increases the thickness of a leaf and hence the flow of nutrients to the leaf.[11] Therefore, iron is an essential element for the growth of plants as well. Iron is one of the most abundant metals in soil and occurs in wide range of chemical forms.[12] Since plants can absorb only certain species,[1] not all of the iron in the soil is available for plants. For example, plants can absorb ferric ions and not ferrous ions.[13] If the pH in the soil is higher than [7], iron ions can be tied to the soil and are not available to plants.[13] Thus, the amount of iron

DOI: here
Reference here

absorption by plants is not merely dependent on the amount of iron present in the soil, but also on the chemical nature of the iron, the pH of the soil and the competition of other minerals. Typical garden soil contains different functional groups such as carboxyl and amines,[1] which interact with ferrous and ferric irons.[14] These interactions may influence the oxidation state and solubility of iron species and hence the availability of iron. However, our knowledge about specific forms of iron occurring in soil and their dependence on various pH values as well as the existence of other minerals is low. Therefore, it is very useful for the scientific community to understand these processes.[1] In this research, we will study the absorption of iron by plants and its oxidation state under different chemical conditions of the soil, to investigate the effect on iron absorption under the presence of competitive minerals in the soil, to understand soil pH dependence of plant iron absorption, and ultimately to gain a better understanding of the soil conditions needed to optimize plant absorption of iron and to help mitigate iron deficiency in the developing world.

Results and Discussion: Plant Anatomy Analysis and Growth Stages. Samples were collected at intervals of two, four, and six weeks. It is shown in Table 1 that the chemical nature of iron species does not change in different regions of the plant due to the fact that the edge energy is all located around 7133eV. This number also indicates both Fe^{2+} and $Fe^{3+}$are present in our samples when compared to the standard Fe-O main edge position. However, the iron level in the roots was the greatest compared to other regions of the plant. On the other hand, the amount of iron varies significantly during different stages of the plant as shown in Figure 1 with U1 being six weeks, having the biggest height difference of 3.7 in absorption coefficient between pre-edge and main edge.[15]

Samples	Amount of Iron (absorption coefficient)	Main Edge Energy (eV)
Soil	170	7133
Roots	149	7133
Mature Leaves	34	7132
Intermediate Leaves	25	7133
Young Leaves	18	7133
Stem (leaf)	17	7133
Stem (trunk)	11	7132

Table 1. Iron Distribution throughout the plant.

Effects of Arsenic and Fe^{3+}. Arsenic and Fe^{3+} were added into the soil of the plants daily. It can be seen from Figure 2 that with the presence of Arsenic in the soil (upper trace), the X-ray absorption is almost flat, indicating the iron absorption is significantly reduced compared to the lower trace without the presence of Arsenic, where iron absorption is obvious. Therefore, pesticides are strongly advised not to be applied during the growth of the plants to enhance the iron absorption. Encouragingly, even in the presence of Arsenic within the soil, the addition of Fe^{3+} helps the plants increase in iron content as illustrated in Figure 3.

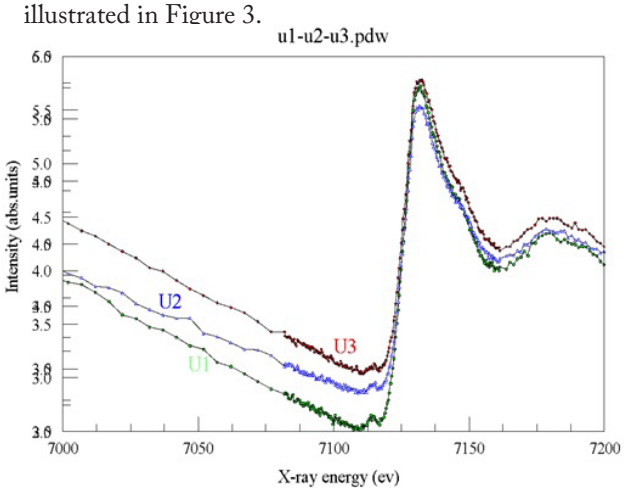

Figure 1. Chemical nature of iron species does not change in different regions of the plant but the amount of iron varies significantly during different growth stages of the plant (U1, U2, U3).

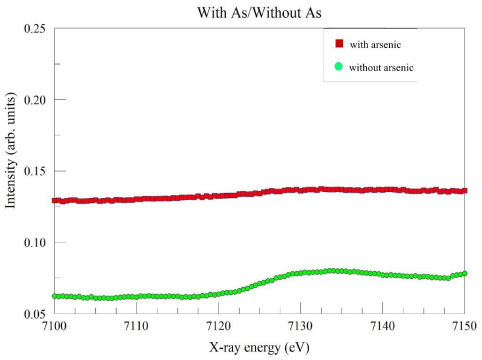

Figure 2. The presence of arsenic prevents the iron absorption of the plants.

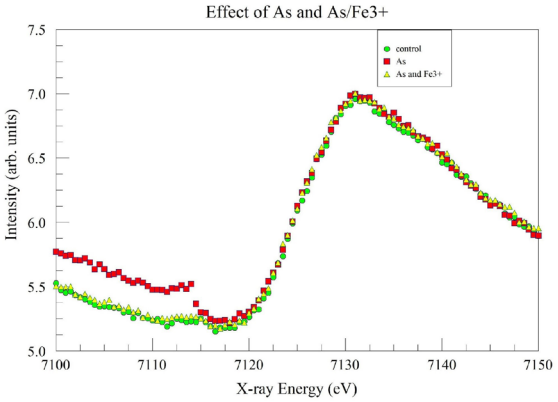

Figure 3. Even with arsenic present in the soil, the addition of Fe^{3+} helps the plants to gain more iron content.

Effects of pH Alterations. $CuSO_4$ and $CaCO_3$ solutions were added to adjust the soil pH and a Kelway soil meter was used to monitor the soil pH values. It is illustrated in Figure 4 that the height difference between the pre-edge and main edge is 0.146624 (control), 0.127592 (pH=7) and 0.196225 (pH=3). In conclusion, lower pH does help the absorption of the iron where the height difference between the pre-edge and main

DOI: here
Reference here

edge is the biggest. On the other hand, higher pH soil prevents iron from absorption.

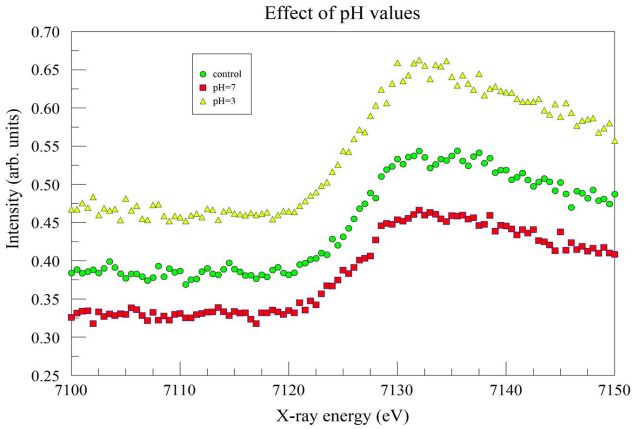

Figure 4. Lower pH (<7) soil helps the absorption of the iron, on the other hand, higher pH soil prevents iron from absorption. The pH of the control was 6.5.

Conclusion. From the present X-ray absorption data, we can conclude that chemical nature of iron species does not change in different regions of *Brassica oleracea* plant. However, the amount of iron varies significantly during different growth stages of the plant. The iron levels in the roots was the greatest compared to other regions of the plant. With the presence of Arsenic in the soil, the iron absorption of the plants is significantly reduced. Therefore, we advise that pesticide should not to be applied during the growth of the plants. Lower pH (< 7) soil helps the absorption of the iron and higher pH soil prevents iron from absorption. With the presence of pre-edge energy, Fe is shown to be bound to oxygen. According to the main edge energy position, both Fe^{2+} and Fe^{3+} are present in our samples, which will be further verified through Mossbauer spectroscopy.

Methods: Sample Preparation. Kale seeds were planted and grown in pots in a greenhouse at Greenwich High School. The green house was at room temperature and the plants were placed in front of several large, light-emitting windows to simulate their natural environment. Samples (soil, leaves, stems and roots of the plant) were collected at different growth stages: 2, 4, and 6 weeks. Samples were then dried at 200˚F and ground to a fine powder form. Equal amounts of samples were sealed in glass tubes to be ready for experiments. Figure 5 are some of the plants grown for this research and Figure 6 shows

Figure 5. Examples of growing plants.

Figure 6. Sample Preparation.

the annealing process to prepare samples.

Instruments and Data Collection. All X-ray absorption data were collected at beam line F3 at Cornell High Energy Synchrotron Source (CHESS). This beam line uses a monochromator with Si (111) crystal to select X-rays of required energy from the white X-ray beam. Intensities of incident and transmitted X-rays were measured using ionization chambers filled with N_2 gas as shown in Figure 7.

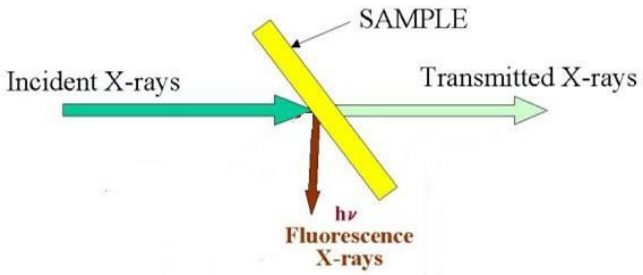

Figure 7. X-ray absorption setup.

Description of the Experiment. X-ray absorption spectroscopy is a technique that is often used to measure the physical and chemical properties of an atom. It is element specific and can be used to study the local environment of an amorphous or crystalline sample. During the experiment, the absorption coefficient of the X-ray was measured as a function of energy through the range of 200 eV below the absorption edge to 1000 eV above the edge. Below the absorption edge, the photons cannot excite the electrons of the relevant atomic level, therefore, the absorption is low. When the photon energy is sufficient to excite the electrons, a large increase in absorption takes place, namely absorption edge or pre-edge. Above the edge, extra energy of the X-rays transfers to ejected photoelectrons in the form of kinetic energy. These photoelectrons can be backscattered by neighboring atoms. The outgoing photoelectrons and backscattered photoelectrons can interfere constructively or destructively, depending on the phase shift, producing oscillations in the absorption coefficient, namely main edge. Generally speaking, the region of the absorption spectrum from 50 eV below the pre-edge to 50 eV above the pre-edge is known as X-ray absorption near edge structure (XANES). The region beyond 50 eV above the main edge is known as Extended X-ray Absorption Fine Structure (EXAFS).[15] Iron in all samples was characterized using XANES and EXAFS in this research. The typical absorption spectrum of a sample containing iron is shown in Figure 8 with 7112 eV for iron K pre-edge. The analysis of these oscillations yields information about iron, such as near neighbor bond length, type of near neighbor atoms, and number of near neighbor atoms. The main

edge position is sensitive to the electron density around iron and therefore changes with the iron oxidation state. In this research, the presence of a pre-edge indicates Fe-O compounds. The main edge energy position is the primary indicator of oxidation state of iron atoms. The intensity difference between the

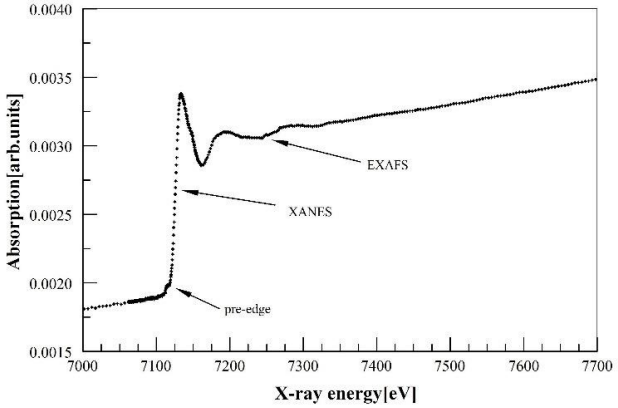

Figure 8. X-ray absorption spectrum of a typical sample of a typical sample containing iron.

pre-edge and the main-edge is proportional to the amount of iron present in the sample.

Acknowledgements. I wish to thank Cornell High Energy Synchrotron Source (CHESS) to allow us to use the facility to perform the experiment. I also wish to thank my teacher Mr. Andy Bramante for his expertise and assistance. I would like to thank my mentor Dr. Sunil Dehipawala from City University of New York for his knowledge and resources.

References.

1. Wessling-Resnick M. Iron. In: Ross AC, Caballero B, Cousins RJ, Tucker KL, Ziegler RG, eds. *Modern Nutrition in Health and Disease.* 11th ed. Baltimore, MD: Lippincott Williams & Wilkins; 2014, 176-88.

2. Aggett PJ. Iron. In: Erdman JW, Macdonald IA, Zeisel SH, eds. *Present Knowledge in Nutrition.* 10th ed. Washington, DC: Wiley-Blackwell; 2012, 506-20.

3. https://en.wikipedia.org/wiki/Vegetarianism

4. https://en.wikipedia.org/wiki/Veganism

5. Waldmann A, Koschizke JW, Leitzmann C, Hahn A, Dietary Iron Intake and Iron Status of German Female Vegans: Results of the German Vegan Study. *Ann Nutr Metab.* **48** (2): 103–108. doi:10.1159/000077045. PMID 14988640, 2004

6. Krajcovicová-Kudlácková M, Simoncic R, Béderová A, Grancicová E, Magálová T, Influence of vegetarian and mixed nutrition on selected haematological and biochemical parameters in children. *Nahrung.* **41** (5): 311–14. doi:10.1002/food.19970410513. PMID 9399258, 1997.

7. Murray-Kolbe LE, Beard J. Iron. In: Coates PM, Betz JM, Blackman MR, et al., eds. *Encyclopedia of Dietary Supplements.* 2nd ed. London and New York: Informa Healthcare; 2010, 432-8.

8. Hurrell R, Egli I. Iron bioavailability and dietary reference values. *Am J Clin Nutr* 2010, 91-1461S-7S. [PubMed abstract]

9. Dietary Reference Intakes for Vitamin A, Vitamin K, Arsenic, Boron, Chromium, Copper, Iodine, Iron, Manganese, Molybdenum, Nickel, Silicon, Vanadium, and Zinc: a Report of the Panel on Micronutrients, *Institute of Medicine (Food and Nutrition Board)*, Washington, DC: National Academy Press; 2001.

10. Gustafsson, I.E; Persson, I; Kleja, D.B; Schail, J.W. Binding of iron (III) to organic soils: EXAFS Spectroscopy and Chemical Equilibrium Modeling, *Environ. Sci. Technol.* 41, 1232-1237, 2007.

11. Glesler, R; Hogberg, M; Hogberg, P. Soil chemistry and plants in Fennoscandian boreal forest as exemplied by a local gradient, *Ecology* 79, 119-137, 1998.

12. Weber, T; Allard, T; Benedetti, M.F. Iron speciation in interaction with organic matter: Modeling and experimental approach, *Journal of Geochem. Exp* 88, 166-171, 2011.

13. Karlsson, T; Persson, P. Coordination chemistry and hydrolysis of Fe(III) in a peat humic acid studied by x-ray absorption spectroscopy, *Geochimica et Cosmochimica Acta* 74, 30-40, 2010.

14. La Force, M.J; and Fendorf, S. Solid phase iron characterization during common selective sequential extraction, *Soil Sci. Soc. Am. J.* 64, 1608-1615, 2000.

15. Sunil D., Pubudu S., Khushpret K. Microstructure of Nickel in Thin Film Magnets Prepared by Spin Coating and Sol gel Techniques, *ASEE Mid-Atlantic spring conference proceedings*, April, 2018

Authors. Cynthia Chen is a junior at Greenwich High School. She has been playing violin for 11 years and is the concertmaster of Principal Orchestra at Norwalk Youth Symphony. Last year, Cynthia launched a renewable sodium-ion battery company, Natrion. Cynthia's experience has led her to consider Biology or Economics as a major.

DOI: here
Reference here

Fecal Indicator Bacteria on Plants in the Fall Kill Creek

Joelle A. Weir[1]*, Chloe Rosa[1], Anointing Akpojetavwo[2]

1. Arlington High School, 1157 State Rte. 55, Lagrangeville, NY 12540, USA
2. Poughkeepsie High School, 70 Forbus St., Poughkeepsie, NY 12603, USA

*joellealexandria@gmail.com

ABSTRACT: The Fall Kill Creek is a tributary of the Hudson River. The Creek is a source of food and a habitat for a variety of animals and other organisms and is used in the community for recreational purposes like fishing and wading. FIB (Fecal Indicator Bacteria), including E. coli and Enterococci, are commonly used to determine water quality. Fall Kill Creek FIB concentrations indicate that there is fecal matter produced from sources such as storm water runoff, septic tanks, and animals within the creek watershed. When Enterococcus levels in the water are equal or greater than 60 MPN (Most Probable Number) / 100 mL, it is considered unsafe for human exposure due to coliforms which indicate a possible presence of disease-causing bacteria.[1] We hypothesize that when plants in streams are disturbed by human activities; biofilms on plants could be dislodged releasing FIB into the water. If plants are contributing to increased FIB levels, this will directly correlate to increased risk of disease from waterborne pathogens.[2] We measured FIB at several sites to test the dependence of FIB on site location, types of plants present, and amount of FIB on the plants. Our results suggest that none of these parameters predict FIB: specifically, there are no differences in numbers of FIB on the different types of plants, there are no differences in numbers of FIB at the different sites, there is no interaction between plant type and site with respect to numbers of FIB, there is no correlation between the amount of FIB on the plants and their concentration in the water. Further research is encouraged, and we advise that subsequent studies might include investigating FIB in sediment to find correlations with the plants. With more time we would also include more plants or sites in the study. The remediation of the Fall Kill Creek has the potential to create a cleaner Hudson River, especially since tributaries often act as a source of pollution. According to the Riverkeeper Annual Water Quality Report, "61% of Riverkeeper's 74 sampling locations in the Hudson River Estuary fail EPA criteria for recreational water."[3] This information is vital for the community and people monitoring the stream quality.

KEYWORDS: Environmental Research; FIB (Fecal Indicator Bacteria); Fall Kill Creek; Hudson River; E. Coli; Enterococcus; Aquatic plants; Biofilm

Introduction. Over the summer of 2018, the MH-YES (Mid-Hudson Young Environmental Scientists) program recruited two science research teams to work at two institutions, Cary Institute of Ecosystem Studies and Marist College. Each team chose a topic in the community to work on that matched the capabilities of their respective institution. The Marist team conducted a six-week long research project on the level of FIB present on plants in the Fall Kill Creek. "The creek has a lot of industrial history, as Poughkeepsie, one of the cities the creek runs through, was a fishing and whale blubber powerhouse in the mid 1900s and earlier. It has defined the economic, environmental, and historical life of the city. In the past 50 years, it has been forgotten, neglected and hidden from residents and neighborhoods in need of vibrant public space." [4] Because of this neglect, the creek has been a dumping ground for waste and trash. Thus, leading us to believe we can trace the footprints of our civilization to FIB and how it presents itself in the Fall Kill Creek's biodiversity. The objective of our research was to find FIB on plants, which is found in the water of the Fall Kill Creek and has settled down onto the submerged sediments in the stream.[5] However, compared to sediments, the total FIB in the water is lower. This is due to FIB's inability to survive in water alone because of competition with other bacteria, as well as temperature and sunlight levels. Since FIB has been known to die in environments where they are not native or well adapted, they live longer in sediments.[2] Thus, our curiosity centered more towards whether the material being colonized by bacteria was plant matter, because studies of sediments surpass the studies of FIBs on plants and there was no research on FIB's presence in the Fall Kill Creek. We conducted our study observing and measuring FIB colonization on different plants in the Fall Kill Creek. Using *E. Coli* - a bacteria commonly found in human waste and Enterococci a group of gram-positive bacteria, we were able to sample different locations along the Fall Kill Creek and conduct a study to find a relationship between FIB in plants and in the water. The amount of FIB in the water varies based on how actively the surrounding community uses the Creek.

Our alternative hypothesis: there is a difference in the number of FIB on the different types of plants, there is a difference in the number of FIB at the different sites, there is an interaction between plant type and site with respect to numbers of FIB, there is a correlation between the amount of FIB on the plants and their concentration in the water.

DOI: here
Reference here

Our null hypothesis: there are no differences in numbers of FIB on the different types of plants; there are no differences in numbers of FIB at the different sites; there is no interaction between plant type and site with respect to numbers of FIB; there is no correlation between the amount of FIB on the plants and their concentration in the water.

Because of the resources and time available to complete this project, we chose methods that kept our team efficient and broadened our knowledge of lab work and protocols.

Results. Was there a difference in the number of FIB on different plants at different sites? (see figures 1 and 2)

- Overall, the Enterococci count recorded was highest at ED on grass sp. and the E. Coli count recorded was highest at UR on grass sp., as shown in figures 2 and 3 respectively. Visually, there seems to be a correlation between high average amount Enterococci and E. Coli on the grass sp. although, the results were not statistically significant.

Is there an interaction between plant type and site with respect to numbers of FIB? (see table 1)

- The results were not statistically significant.

Was there a correlation between the amount of FIB on the plants and their concentration in the water? (see figures 3 and 4 below)

- Although there was a trend on the graph to suggest a difference, there was no difference between plant type or sites and no correlation between amount of FIB on the plants and their concentration in the water based on a 2-way ANOVA test. It is concluded that the P-value was not strong enough to show correlation.

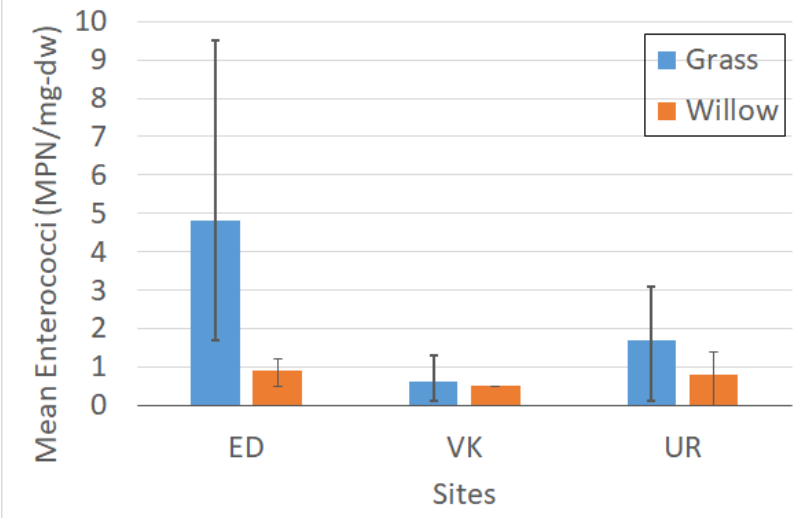

Figure 1 depicts mean of Enterococci on grass sp. and willow sp. at all three sites along the Fall Kill.

Using a Two-Way ANOVA, performed on ranked data of Enterococci and E. coli plant species and sites, resulted in $p > 0.05$ for all plants, sites, interactions and a correlation between plants and water under enterococci and E. coli.

Discussion. Since the results were based on an observation across 2 plant types, 3 locations and 3 trials per plant, one can propose to copy this observation with more plants, more sites and more trials. As well as this, one might consider classifying

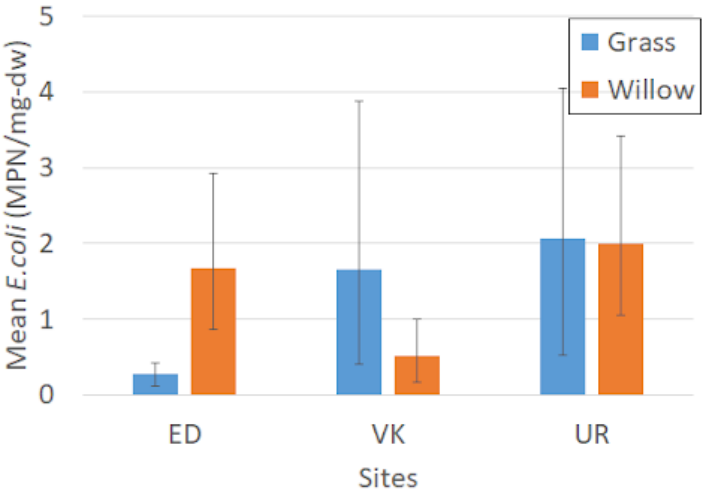

Figure 2 above depicts mean E. Coli on grass sp. and willow sp. at all three sites along the Fall Kill.

	Enterococci	*E. Coli*
Plants	0.077	0.486
Sites	0.175	0.071
Interatction (plants x sites)	0.445	0.054

Table 1 shows the p values for FIB tested.

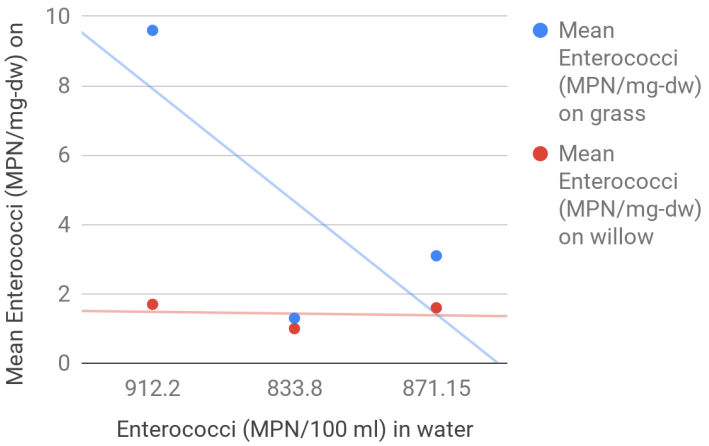

Figure 3.

the plants more specifically in terms of genus and family. Also, when collecting for our positive control, all the wells fluoresced when testing for Coliforms; thus, the Coliforms could not be measured given the type of Quanti-Tray used with the IDEXX System.[6] A larger Quanti-Tray would have been acceptable for this amount of bacteria. Also, when counting wells fluorescing, some might be more apparent than others. It is strongly recommended that the same individual team member counts the fluorescing wells for the purpose of consistency. The Quan-

DOI: here
Reference here

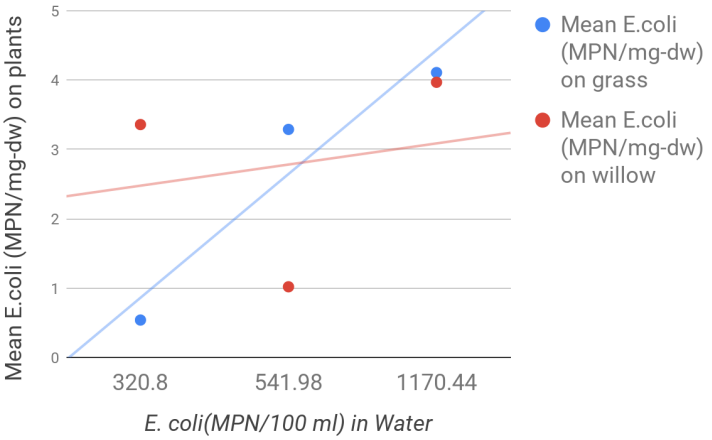

Figure 4.

ti-Tray the Marist Team used was a 97 cell Quanti-Tray/2000 plate. If subsequent studies were to follow, we suggest broadening the scope of what might affect the amount of FIB on plants. For example, investigating sediment to find correlation with plants, the time of day plants are observed/collected, increasing the sample size, add new sites and/or plants, using a bigger sample, obtaining a sample of water before and after disturbed by people within a set perimeter and even observing plants through different seasons.

Our overall findings may not suggest a difference in FIB; however, our observations of water quality and the creek's ecosystem suggest remediation of the Fall Kill creek would be recommended to keep the community safe. A wastewater treatment plan should be implemented, with an emphasis on residential participation. This may incorporate the education of the surrounding community including organized cleanups, science programs aimed at the study of the water's ecosystem, as well as a guide on how to use the Fall Kill Creek in a way that is efficient and does not harm citizens.[4] Runoff and overflowing water from the Hudson Valley septic tank has been a huge contribution to FIBs, especially Combined Sewer Overflow (CSO) caused by home septic tanks overflowing with rainwater and flowing into the Fall Kill Creek. (Seen in the guide as "Drinking water.")[4] In an effort to reduce waste related pollution, residents of Poughkeepsie should adopt green infrastructure practices like soil and vegetation on rooftops or rain barrels to capture stormwater runoff. Through these activities, the community comes to admire how much the Creek provides for them economically.[4]

The Fall Kill creek, a known tributary to the Hudson River, has the potential to create a cleaner Hudson River, especially since tributaries often act as a source of pollution.[3] Enacting these remediations on the creek will create a cleaner community and a greater resource to the people of its community and in a perfect world, the Hudson River might even get the same treatment to promote cleanliness. Riverkeeper, an advocate organization for New York's clean water, run by Robert Kennedy until 2017, creates annual water quality reports to update the public about water safety in their communities. Their latest report outlined key details in the state of the Hudson River, including the fact that "23% of Riverkeeper's samples failed safe-swimming guidelines" and "61% of Riverkeeper's 74 sampling locations in the Hudson River Estuary fail EPA criteria for recreational water"[3] and were followed by remediation techniques promoted by Riverkeeper. However, "Dutchess County samples water quality here weekly, the minimum recommended by the EPA, but does not routinely make testing results public.",[3] thus, the counties surrounding the river, mainly Dutchess and Ulster, need to make the state of the Fall Kill creek known to the public and obtain an updated roster of recreational activities that are safe for civilians.

Our research can be used as a precedent for scholarly research pertaining to water quality as well as an example for spreading valuable information about the Fall Kill creek to the people who live in its vicinity. Residents were intrigued by our research stemming from the fact that we needed to access the land through public and private property, which attracted attention to our work. This impacted our research by not only improving our understanding of the ways that the creek had become polluted but also how it is an asset to the community.

Conclusion. The results mean accepting all the NULL hypotheses and concluding that there is no significant difference between the amount of FIB on grass and willow, there is no significant differences in the amount of FIB at each site; there is no interaction between plant type and site with respect to the amounts of FIB, there is no significant correlation between the amount of FIB on the plants and their concentration in the water. There was no indication in our research that FIB levels on plants directly contribute to the high levels of FIB in the water or result in reducing FIB levels in the water.

Methods. In order to determine whether fecal indicators are detectable on the plants' biofilm in the Fall Kill, the Marist Team measured FIB on willow sp. and grass sp. at three sites along the Fall Kill Creek: East Dorsey (ED), Val-Kill (VK) and Upper Roosevelt (UR) in Hyde Park, NY. These sites were chosen based on accessibility, whether both plants were there and whether plants were submerged or not. East Dorsey was in a suburban area and located in the backyard of many residents and was closed off more than any other. Upper Roosevelt had the most diversity but lacked easy entry on foot because of the remote location. Val-Kill was the only location in a public space often used for recreation and the most accessible.

Figure 5. Val-Kill.

Figure 6. East Dorsey.

Figure 7. Upper Roosevelt.

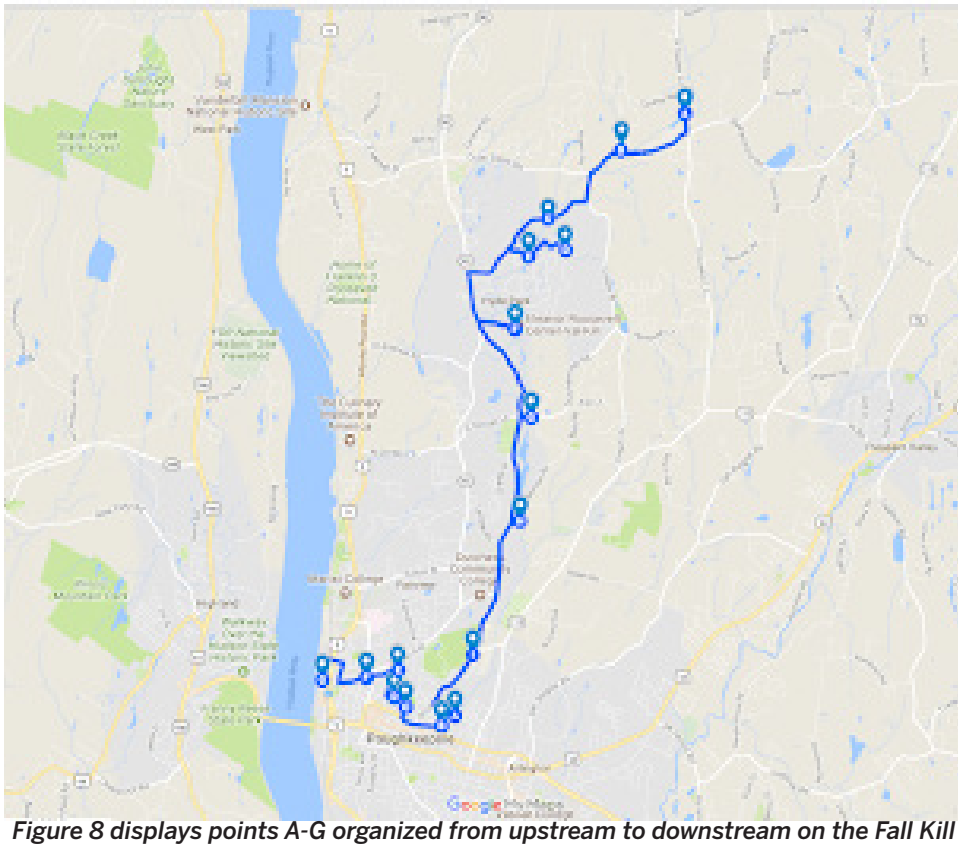

Figure 8 displays points A-G organized from upstream to downstream on the Fall Kill Creek. Points G, F, and D are ED or East Dorsey Lane, VK, and UR or Roosevelt Lane respectively.

Method to Expel Bacteria. We used a vortex and homogenizer to expel bacteria from our samples, because other methods (e.g. ultrasonic probe and sonic bath) could have destroyed our bacteria in the biofilm on our plant samples. [7]

Field Protocol. When in the field, a perimeter of ten meters along the bank of the creek and at the width of ED, VK, and UR respectively was made. The total surface area for each location was made at a perimeter of 19.6 meters^2, 97.8 meters^2, and 37.2 meters^2 respectively. Once a perimeter was set, *willow sp*. and *grass sp*., were located within the box and we measured their respective lengths and widths to find the surface area of the plant replicates at the determined location. At ED, the surface area of grass was made at a perimeter of 1.2 meters^2 and willow at 8.9 meters^2; At VK, the surface area of grass was made at a perimeter of 16. 6 meters^2 and willow 5.9 meters^2; At UR, 1.7 meters^2 and willow 4.9 meters^2. We calculated the area of the total perimeter as well as the area for the *willow sp.* and the *grass sp*. to make up the total perimeter. After determining both plant species' areas for the individual sites, we collected four replicates of willow sp. and grass sp., and a water sample measuring conductivity, dissolved oxygen, total dissolved solids and temperature at each site. To collect the plants, we went into the Fall Kill with waders and used forceps to place in one Whirl-Pak bag. Each bag was designated for one plant species per plant site. We then, located our plants and had to reach under the water in order to acquire the submerged plants. After that, we detached the leaves from the stem using forceps and put four replicates in the Whirl-Pak bag, sealed the bag and then labeled the time collected, type of plant, who got it, and which site it came from. Finally, the replicates were put into the bag in the cooler with the water samples, ensuring it would not be disturbed by the summer heat.

Running Positive and Negative Controls. Using no plants or fecal indicator bacteria, deionized water was placed in a Quanti-tray. Only one small well fluoresced amounting to 1 MPN/100 mL: our negative control. Using homogenized fontinalis in deionized water (see homogenization protocol), we found 48 large wells and 21 small wells in the Quanti-trays amounting to 285.1 MPN/100 mL: our positive control. This confirmed our suspicion of FIB being present in the Fall Kill Creek from our sample species from the Fall Kill.

Lab Protocol. Diluting Saline Solution.*The stock solution is made up of PO43 (phosphate) buffered saline solution (PBS)

- In order to get rid of excess FIB in stream water on the leaves, we had to create a solution made up of 10% stock

DOI: here
Reference here

ED	Wet weight	Dry Weight	TIME STAMP
Sample Rep1 Rep2 Rep3	.081 g .079 g .082 g .168 g	.008 g	2:20 pm
VK			
Sample Rep1 Rep2 Rep3	.303 g .566 g 1.047 g 1.344 g	.013 g	2:31 pm
UR			
Sample Rep1 Rep2 Rep3	.521 g .296 g .633 g .223 g	.048 g	2:28 pm

Table 2 shows an example of how to record the weight of a plant leaf.

solution and 90% deionized water with a fluid total of 12000 mL (12L). Due to the number of bottles available, we only made about 6000 mL at a time.

- First, we created the stock solution. [8] Next, we collected deionized water in 7x 1000mL Erlenmeyer flasks filled to 675 mL deionized water and then set to autoclave. After about 3 and a half hours of autoclaving, we poured 75 mL of stock solution in a graduated cylinder. One cannot fill the flask all the way because of the pressure of the autoclaved deionized water, thus, it is recommended to fill up ¾ of the bottle.
- When storing, we placed a cap on the Erlenmeyer flask so no new bacteria could contaminate the solution.
- Repeat and get a leftover of 1350 mL deionized water and 150 mL of stock solution, then split into 2 bottles (675 mL and 75 mL in each). Total: 16 Erlenmeyer bottles of saline solution.

Weighing wet sample

- First, trays were labeled with the date, sample species, site, sample, and initials of handler. (E.G. - 7/19, *willow sp.*, VK, sample, C.R.). Next, the trays were put onto a scale and "T", for tare, was pressed so the weight of the tray was not added to the mass of the plant leaf. Once the scale is reset to 0, after "T" is pressed, the replica was taken from the Whirl-Pak bag and onto the scale. The weight was then recorded in grams and placed into the incubator for about 24 hours. After 24 hours, weighed dry sample was placed with the tray with on the scale. Then, lifting the plant leaf up with forceps, the weight of the tray was tared and then placed back onto the scale with forceps. The weight was then recorded in grams.

Cleaning replicates

- In order to clean replicates, disposable gloves were put on and sterilized forceps were used to take the replica from the Whirl-Pak bag and to hold the plant leaf replica at one end. The forceps were then used to dip the replica into container 1 of 50 mL of 10% saline solution and then dipped again into container 2 of 50 mL of 10% saline solution. The "dip" was a slow motion, thus, not disturbing the FIB on the biofilm of the replica leaf. This method was repeated three times for each replica.
- Once a replica is dipped, the sample was held above a paper towel (disposed into bio-waste bag later) to be stripped of excess moisture. Next, the replica was gently placed into 50 mL centrifuge tube filled with 30 mL of 10% saline solution, cut into pieces and placed to be homogenized.
- The fourth replica was the standard measure of weight for that species from that location.
- After containers 1 and 2 were used three times per plant species at a specific site, they were thrown into a bio waste bag to be autoclaved and disposed of properly (See weighing wet samples).

Cleaning homogenizer. The homogenizer must be cleaned before and after use.

- When homogenizer is cleaned, working over a beaker to collect liquid, using alcohol on the homogenizer is preferable. The homogenizer was sprayed with alcohol and then ran for 20 seconds. Then, the homogenizer was wiped with a Kim Wipe and checked for plant matter. If there was said plant matter, it was removed with sterile forceps (forceps sterilized with alcohol). This process was repeated until all plant matter was removed and the homogenizer was dry.

Isolating bacteria

- Plant leaf samples were rinsed gently by dipping into sterile PBS solution before being placed into 50-mL centrifuge tubes containing 30 mL of PBS (see cleaning samples protocol).8 The leaves were then cut into small bits and homogenized (or until the liquid looks like a tinted green

color for both species of submerged plant) and then vortexed. Homogenizer was cleaned thoroughly and checked for plant matter. Once the leaf samples were fully blended, 15 mL of those samples from the centrifuge tube was added to an IDEXX container (Colilert) and the other 15 mL measurement from the centrifuge tube was added to another IDEXX container (Enterolert). Then, an additional 85 mL of 10% saline solution was added to both IDEXX containers. (See saline solution protocol). The IDEXX containers were then shaken until both IDEXX solution dissolved into the container. The content of the IDEXX container was then poured into Quanti-trays, put through the Sealer, and then labeled with site, date, sample species and replicate, initials of person handling the Quanti-tray, time incubated, and whether the Quanti-tray will detect enterococci or coliform bacteria. The Quanti-tray detecting Enterococcus went into a stainless-steel incubator at 41 degrees Celsius. The Quanti-tray detecting E. Coli went into an incubator at 35 degrees Celsius.

Quanti Trays & IDEXX System. Fecal Coliforms were among the FIB present in the Fall Kill Creek and were indicated using Enterococci and E. coli in our research proposal.

Submerged plants. The topic of submerging plants was an important factor since the results are impacted by the amount of FIB on the biofilm of plant leaves in the creek. Due to a week of rain in July, our results may have been impacted as rain introduces more bacteria into the creek. However, what was not accounted for was the elevation of water, thus, causing plant leaves that were not submerged to become submerged. As a result, methods were changed from taking just a submerged plant leaf to a plant leaf submerged in at least 30 cm of water.

Surface Area vs Weighing. Our team decided to record the plants in mg instead of surface area (cm^2). What was not considered was standardized mass across both plant samples of *willow sp*. and *grass sp*. ex: collecting the same weight for both species instead of collecting roughly 10 cm of each sample of each plant at each site. Instead of standardizing all the weights, we took one sample, dried it, then used the dry and wet weight of the sample as a proportion to find the replicates' dry weight.

Range of Time to Collect Plants: collegting plants in the field. The team collected the *willow sp*. and the *grass sp*. two days apart. Both collections were left to sit for about 24 hours before processing them. Thus, there was a concern that a stationary Whirl-Pak bag could induce either bacteria growth

Plant Species	Date	Site	Replicates	Mass wet (mg)	Wet/Dry weight	.5 Dry Wt. (mg) (Mass wet/(wet /dry))/2	MPN/100 mL Enterolert-Enterococci	MPN/100 mL Colilert-*E. Coli*	Enterococci (MPN/mg-dw)	*E.Coli* (MPN/mg-dw)
Willow	7/31/18	UR	1A	236	7.76	15.2	19	16	1.2	1.1
			1B	307	7.76	19.8	11.5	10.9	0.6	0.6
			3A	208	7.76	13.4	16.4	26.5	1.2	2.0
			3B	130	7.76	8.4	26.3	6.3	3.1	0.8

Table 3 shows plant leaf processed 3 hours later.

Plant Species	Date Collected	Site	Replicates	Mass wet (mg)	Wet/Dry weight	.5 Dry weight (mg)	MPN/100 mL Enterolert-Enterococci	MPN/100 mL Colilert-*E. Coli*	Enterococci (MPN/mg-dw)	*E. Coli* (MPN/mg - dw)
Willow	7/31/18	UR	1A	373	7.76	24.0	1.0	9.6	0.0	0.4
			1B	299	7.76	19.3	4.1	24.9	0.2	1.3
			3A	147	7.76	9.5	6.3	6.3	0.7	0.7
			3B	284	7.76	18.3	4.1	5.2	0.2	0.3

Table 4 shows plant leaf processed 30 hours later.

DOI: here
Reference here

or decay during the 24 hours. To test to see if bacteria increased or decreased based on how long the samples were stored, we went out to collect *willow sp*. at the UR site. Both samples were collected around noon. We did this procedure twice for 4 samples (including dry weight sample and 3 replicates) one day apart for each collection. Table 1 records samples processed 3 hours later. Table 2 records samples processed 30 hours later.

We predicted that there would either be:

- A clear difference (Alternative Hypothesis) or
- No difference (Null Hypothesis)

$$VAR_3 = VAR_{30}$$

*mg-dw = milligrams of dry weight

Based on this data, we used statistical analyses to determine our predictions in the amount of MPN/100 mL Enterococci and *E. Coli*. The data was ranked. The natural log was taken to standardize the variances.

This resulted in the information being entered into Excel and performing a 2-way ANOVA on the ranked data as well as an F- test to find equal variance in samples processed 3 hours later and 30 hours later.

If P < 0.05, then we reject the NULL HYPOTHESIS because there is a significant difference in the amount of time between processing plants.

Actual Results:

P<=.06308394586 did not change for Enterococci

P<=.3273723005 did not change for *E. Coli*

Given the two tailed P-values, indicating if either result of MPN/100 ML increases or decreases based on the amount of time before processing, we fail to reject the null hypothesis. This means we can compare grass collected up to 30 hours from extraction to grass collected 3 hours from extraction.

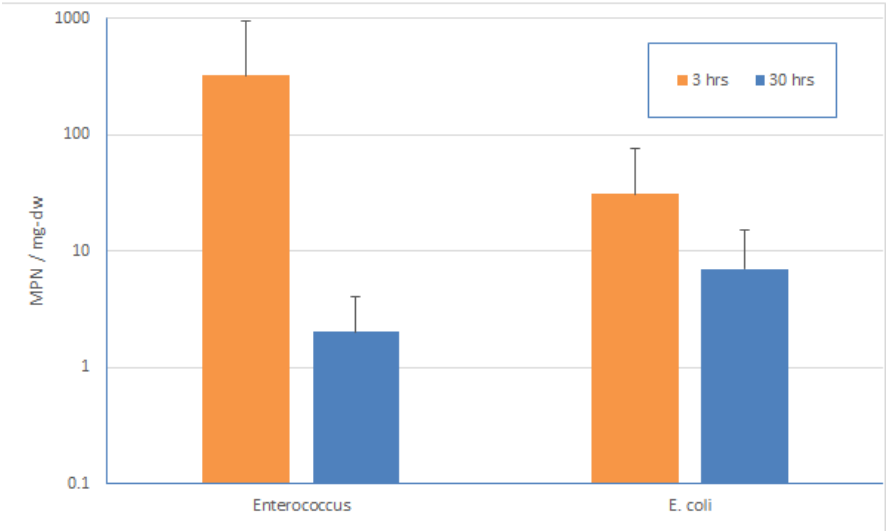

Figure 9 depicts Enterococci and E. Coli results formed 3 hours later and 20 hours later averaged.

Acknowledgements. This research was achieved through the MH-YES (Mid-Hudson Young Environmental Scientists) program, funded by Cary Institute of Ecosystem Studies as well as Columbia University and supported by Marist College. We thank our mentors and teachers Ashana Neale, Dr. Raymond Kepner, Michael Gendler, Dr. Rhea Esposito, and Dr. Richard Feldman who provided insight and expertise that greatly assisted the research.

As the author, I would like to thank my editors Margaret Ruth Lindeman, Tricia Muracoi, Brianna Porter and Rita Rabadi who gave their time and writing skills to help compose this paper.

Thank you to my research partners Anointing Akpojetavwo and Chloe Rosa for making the research fun and doable. Team work makes the dream work.

Bibliography.

Bauer, TW; Fujishiro, T; Kobayashi, N; Procop, GW; Tuohy, MJ; etc. *The Effect of Ultrasonication On the Detention of Bacteria in a Biofilm.*

References.

1. (2012) Recreational water quality criteria. United States Environmental Protection Agency. https://www.epa.gov/wqc/2012-recreational-water-quality-criteria

2. Kepner, Dr. Raymond; Johnson, Timothy C. (2015) *Hudson River Sediment as a Reservoir for Potentially Pathogenic Bacteria.*

3. (2014). Riverkeeper's annual water quality report. *Riverkeeper, Inc.* https://www.riverkeeper.org/water-quality/testing/

4. Palmer, Ryan; Kim, Janette; etc. (2012). *A user's guide to the fall kill creek. Hudson River Sloop Clearwater*. pp. 12-15. https://www.clearwater.org/pdf/HANDBOOK_spreads_Optimized.pdf. 2019. Mar. 1

5. *Water Res.*(2014);61: 276-87. doi: 10.1016/j.watres.2014.05.007. Epub 2014 May 27. 2019. Mar. 31

6. Yakub, Gary P; Castric, David A.; Stadterman-Knauer; Kathleen L.; etc. *Evaluation of Colilert and Enterolert Defined Substrate Methodology for Wastewater Applications. Water Environment Research* .2002.74. pp. 131-135

7. Buessing, Nanna; Gessner, Mark O.(2002) .*Comparison of detachment procedure for direct counts of bacteria associated with sediment particles, plant litter and epiphytic bio films. A M E*, 27, pp. 29 - 36.

8. Harley, J.P. (2014). Laboratory Exercises in Microbiology (9th Edition), *McGraw-Hill Publishing*, New York, NY, pp. 421+ appendices.

Authors. Joelle Weir is currently a senior at Arlington High School who's always found science and mathematics the highlight of her academic years. When presented with the opportunity to start her career in STEM early and work with the MH-YES program, she welcomed the idea and became a Science Researcher in the summer of 2018. Since then, she and her teammates were featured at several seminars promoting community engagement in STEM and Joelle has taken a scientific research class at Arlington to further her understanding in research. She is interested in majoring in Data Analytics or Environmental Engineering. She plans to attend the University of Toronto in the fall.

"I'm excited to present this as part of the first group to research surrounding the topic of Fecal Indicator Bacteria present on plants questions in the Hudson Valley." - Joelle Weir.

Chloe Rosa is currently a senior at Arlington High School and plans to major in marine biology and is hoping to attend school outside of New York after attending community college.

Anointing Akpojetavwo is currently a senior at Poughkeepsie High School and plans to major in Biomedical Sciences or double major in Physical Science and Engineering. His schooling after high school will potentially be in the United Kingdom.

INTERNATIONAL RESEARCH COLLABORATIONS

Are you interested in bringing your students' independent science or math research to a higher level?

Are you convinced that research experiences for students must replicate the collaborative nature of science research as it is practiced in the 21st century?

Are you convinced that international collaboration and communication are key components to creating cultural and scientific intelligence?

Terra announces the creation of a new and unique program that features opportunities for participating schools to engage in a scientific and cultural exchange between schools in different countries. The collaborations will be patterned after the long-running programs between American, South Korean, and Singaporean students as featured in Nature in 2015.

Program Summary

The project is initiated by an initial school visit by faculty mentors and students.

Collaborative student research continues throughout the school year with guidance from faculty mentors.

During the final visit, data is analyzed, presentations prepared and ultimately presented in an "endpoint presentation" such as participation in Genius Olympiad.

Terra will assist in setting up high school partnerships, logistical support, consultations on program setup, staff training, and other need based assistance.

Terra can provide professional development on setting an Independent Research Program.

IRC

For more information, visit internationalresearchcollaborations.org

IJHSR International Journal of High School Research

The International Journal of High School Research seeks to publish the highest quality of student work through a peer-review process by university faculty members to represent the future of the scientific community.

If you would like to see your work published here, send your research to editor@terraed.org

High school students from any country can submit their research to be considered for publication if they have received an award at their local science fair.

Why publish with IJHSR?

Students gain experience writing for a scientific journal which may help their college applications stand out. IJHSR is unique in that high school students from around the globe are published together. Students can see how they stack up internationally and read the work of their worldwide peers.

for more information, visit ijhighschoolresearch.org

The International Journal of High School Research is published
by Terra Science and Education